Thesis for the Degree of Licentiate of Philosophy

Multivariate Quality Control and Diagnosis of Sources of Variation in Assembled Products

Kristina Wärmefjord

CHALMERS | GÖTEBORG UNIVERSITY

Department of Mathematical Statistics
Chalmers University of Technology and Göteborg University
SE-412 96 Göteborg, Sweden
Göteborg, Sweden 2004

Multivariate Quality Control and Diagnosis of Sources of Variation in Assembled Products
KRISTINA WÄRMEFJORD

ISSN 0347-2809/No. 2004:27
Department of Mathematical Statistics
Chalmers University of Technology and Göteborg University
SE-412 96 Göteborg, Sweden
Telephone +46 (0)31-772 1000
Göteborg, 2004

Multivariate Quality Control and Diagnosis of Sources of Variation in Assembled Products

KRISTINA WÄRMEFJORD
Department of Mathematical Statistics
Chalmers University of Technology and Göteborg University

Abstract

Variation in key geometrical characteristics in assembled products is a usual problem in automotive and other industries. Geometrical variation and its causes and effects are described and different methods to reduce this variation are considered.

In order to control the variation, a control chart is traditionally used to detect if the process is out of control and therefore should be adjusted. However, some of the variation is very difficult to eliminate at a reasonable cost. Therefore, a quality system that allows for trends in the processes as long as the produced items are within specifications is introduced. This is done by using traditional charts to improve low capability processes, while high capability processes are controlled by acceptance control charts, in order to see that the produced items still are will within specifications.

If a variation is detected it is essential to find the root cause of the problem. Different methods for root cause analysis are applied to industrial data and their performances are compared. Methods for multivariate statistical process control are also considered. The most successful method for root cause analysis is based on a sensitivity matrix. This matrix relates the movements of the inspection points to those of the locators.

Keywords: geometrical variation, quality control, acceptance control charts, multivariate statistical process control, root cause, rigid body, fixture diagnosis

Acknowledgements

My personal thanks goes to:

My supervisor Johan Carlson for his enthusiasm, support and encouragement throughout this work.

My second supervisor Jacques de Maré, who has read the manuscript and provided valuable comments.

Everybody who helped me and supported this work at Saab Automobile AB, in particular to the members of the working group: Johan Vallhagen, who has also been my supervisor at Saab, Magnus Arnér, Tommy Egelström, Anders Green, Christer Jonsson, Peter Josefsson, Christian Karlsson, Niklas Nylén and Hans-Olof Svensson and to the members of the steering committee: Bo Anulf, Morgan Fransson, Stephen Harrison, Jon Höglind and Håkan Larsson.

Rikard Söderberg, also member of the steering committee, and his colleague Lars Lindkvist at the Department of Product and Production Development at Chalmers, who let me use their software RD&T.

Mattias and the rest of my family for their support. Especially to Annika and Thomas for taking care of my horses when I do not have the time.

Contents

Chapter 1

Introduction

This work is a part of a two-year long project between Saab Automobile AB, Chalmers University of Technology and Fraunhofer Chalmers Research Centre. It aims to develop principles, working procedures and tools for finding fixture related root causes of geometrical variation in assembled products. The work is contained in a research project, called "Three Dimensional Tolerance Management" (3DTM), going on at Chalmers. It deals with methods for minimizing geometrical variation in assembled products.

The thesis is divided into three major parts. The first part is this introduction, where general ideas and principles concerning geometrical variation in assembled products are considered. The introduction gives the motivation of the methods described in later chapters, and it also gives a basis for concepts and ideas used in those chapters.

In the remaining two parts of the thesis, topics related to geometrical variation are discussed; namely how to detect variations and deviations using statistical process control and how to identify root causes of the variation. In Chapter 2 a suggestion of how to use process control in order to get a process able to meet specifications is given. This means that an acceptance chart can be used to control a stable process with high capability, while a traditional control chart is used to improve a process with low capability.

The last part of the thesis, Chapter 3, contains a study of methods used for multivariate statistical control and methods for root cause analysis of geometrical variation in assembled products. The methods are applied on case studies and their performances are compared.

The methods described are tested on data from automotive industry. However, most of the methods should be applicable to any kind of rigid assembled product, provided that key geometrical characteristics of the product are measured.

1.1 Goal of the project

The goal of the project is to develop and adopt methods for process control and diagnosis that support a tool based on geometrical inspection data, which may be used in everyday work with the assembly processes. The tool shall

- Be easy to use and enable quick identification of root causes in complex assemblies.
- Translate variations and deviation in geometric data to adjustable process parameters.
- Make it possible to simulate and verify the effects of actions taken in the process.
- Be a support in evaluation of different inspection point layouts.

1.2 The assembly process

In order to discuss geometrical variation, considered in Section 1.5, it is crucial to have a knowledge of the assembly process, which is described in this section.

The position of inspection and positioning points are described using a coordinate system of the car. A point on the car body is completely determined by its coordinates. The coordinate system comprises three mutually perpendicular planes, where:

- The X axis runs in the longitudinal direction of the car, with its origin in front of the car.
- The Y axis runs in the transverse direction of the car, with its origin in the centre line of the car.
- The Z axis describes the height in the car.

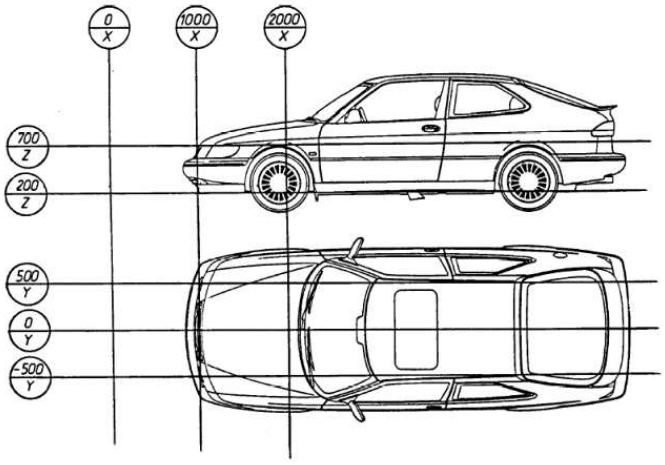

Figure 1.1: *The coordinate system of a car, Saab standard (28)*

The coordinate system is illustrated in Figure 1.1.

To position a part or subassembly during assembly and inspection a positioning frame (P-frame) is used. In automotive industry a 3-2-1 locating scheme is a usual choice to lock the six degrees of freedom of a part. Three master locating points, usually called $A1$, $A2$ and $A3$, are used to form a plane locking one translation and two rotations, two points, $B1$ and $B2$, lock one translation and one rotation and the last point, $C1$, lock the remaining translation. The part is assumed to never loose contact with the locators. This is illustrated in Figure 1.2. The part is positioned in its fixture or joined to another part by bringing its P-frame in contact with a mating P-frame on the target, see Figure 1.3. In addition to the master location points, supplementary points can be required to provide a complete guidance of a part, due to slenderness or spring back factors. Planes, holes and slots are used to represent the locator points in practise.

The selection of master location points is in high extent based on experience, but there are some guidelines in Saab standard (27);

- The manufacturing variations within restricted master location surfaces shall be possible to regard as negligible.

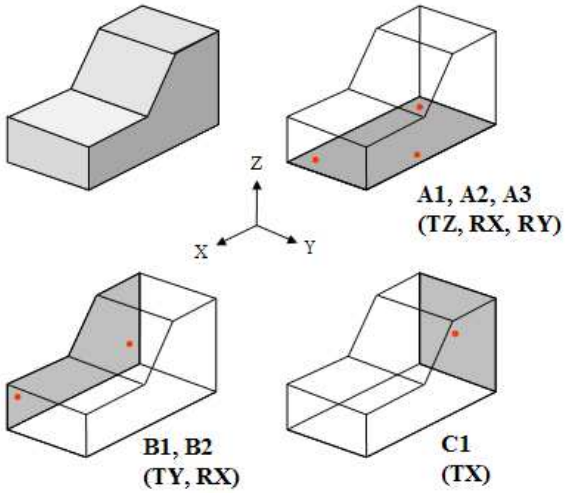

Figure 1.2: *A 3-2-1 locating scheme, Söderberg and Lindkvist (30)*

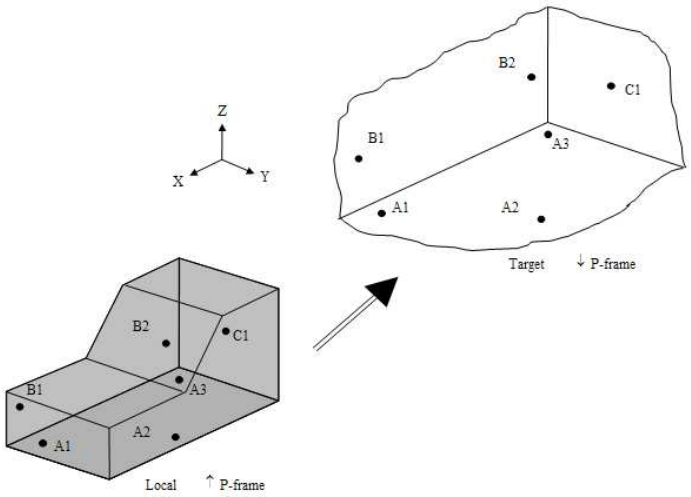

Figure 1.3: *Positioning of a part using 3-2-1 locating scheme, Söderberg and Lindkvist (30)*

- The master location points on mating parts shall, if possible, be positioned directly opposite each other.
- The master location points shall be selected so that the locating features permit accessibility of welding equipment and assembly equipment.
- The range of the master location points on a coordinate shall be as wide as possible.

A complete car is made up of many subassemblies. In every assembly step, it is crucial that the parts are joined with as good precision as possible. This is supported by a robust locating scheme, i.e. a positioning that suppresses variation in the resulting assembly. However, there is always variation between the local P-frame and the target P-frame, and this variation propagates through the assembly. When the assembly is measured, this variation will be detected. At this stage, it may though be a difficult task to identify the root cause of the variation. This is illustrated in the following example. Consider the assembly in Figure 1.4. It consists of two parts, and both parts are positioned using a hole and a slot. The parts are joined and finally measured. The inspection points are represented by arrows in Figure 1.4. The arrows indicate the evaluation direction. Hence, only the deviations in the indicated directions are determined. During the inspection process the assembly is positioned using hole P1 from Part 1 and slot P4 from Part 2. If there is variation in P4 during assembly this perturbation will result in a departure from nominal in the inspection points as shown in the figure. Considering inspection data only, it is not obvious what caused the deviation.

It is important to realize that if there is variation in P4, the only way to achieve a correct assembly is to reduce this variation. If there is a deviation in P4, there are two possible corrections opportunities. The first is to correct the position of P4. The second one is to compensate the deviation in P4 by moving the positions of the locators P1, P2 and P3.

1.3 The inspection process

To detect deviations and variations in parts and subassemblies it is necessary with a continuous control of the processes. The inspection data, used for this purpose, belong to one of two categories; ungrouped or grouped data. The ungrouped data, also called "one at a time"-data, come from inline measurements. An example of inline data can be seen in Figure 1.5. The measurements come from parts produced after each other. Every item

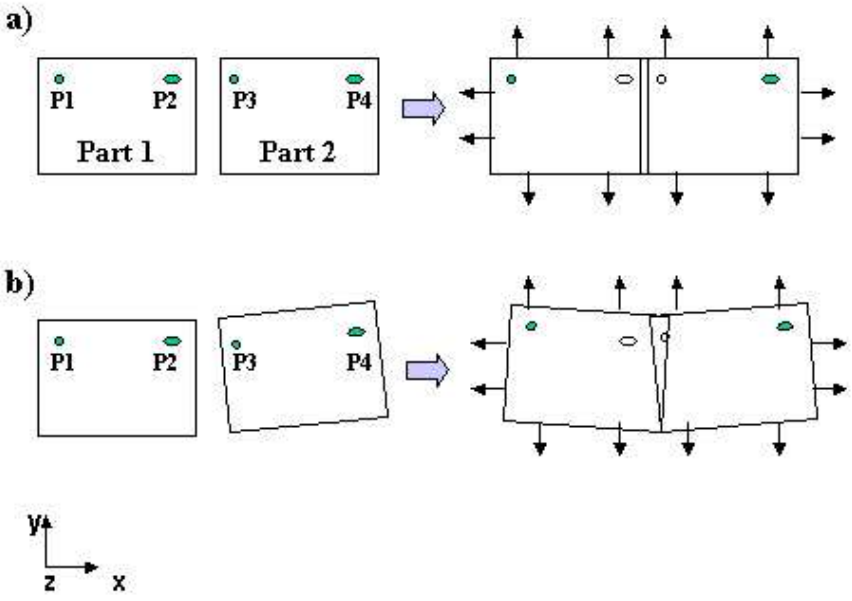

Figure 1.4: *An assembly consisting of two parts. In a) the parts are positioned correctly, in b) there is a perturbation in locator P4.*

produced in a line containing an inline measurement machine is measured as a stage in the production line.

The grouped data consist of samples of n items each. At Saab, a sample size of $n = 3$ is used. These samples are usually taken once or twice a week and the items are measured in coordinate measurement machines (CMMs). A CMM can be seen in Figure 1.6.

In Figure 1.7 an example of CMM data is given. Compared to the inline data in Figure 1.5, those data are sampled during a much longer period of time. There are often trends and long-term variation in a typical process. Much of this long-term variation is not included in the inline data, which are measured during a day or two, but can be seen in the plot of the CMM-data, that are collected during several months. In this example, a sample size of three observations is used. A larger sample size would of course give more accurate information about the process but this must be weighted against an increased cost.

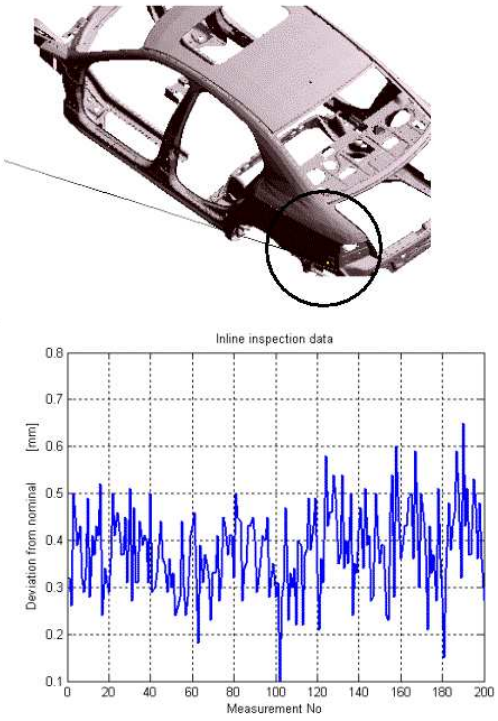

Figure 1.5: *In the top of the figure the inspection point in question is encircled. Below, an example of inline data for this inspection point is plotted. There are 200 items measured.*

The sampling frequency is a question related to the sample size. The frequency should depend on how quick the process may be expected to change, Montgomery (25). If the process may be assumed to vary quickly the sampling should be more frequent then if the process varies slowly. A process that is essential to the final product should be sampled more frequent then a process that only give a minor contribution to the final result. However, just as with the sample size, this issue is a question of balance between costs for inspection and costs for undetected changes in a process.

An inline measurement machine uses laser beams to measure possible

Figure 1.6: *A front fender is measured in a CMM.*

deviation from the nominal coordinates of a point. The measurements have a good precision, i.e. there is a high degree of conformity between independent measurements under the same conditions. The agreement between real value and the value given by the measurement machine, i.e. the accuracy, is lower than for a CMM. Inline measurements are though valuable since they give continuous information about the process. However, while every produced item is measured, it is too time consuming to measure as many points as in the CMM's. There is also some lack of accordance between the CMM and the inline measurements. The CMM is considered as the more reliable measurement device. It is important to be aware of the possible drift in the inline measurement machine and first and foremost use it as a tool for detecting increased short-term variation.

The inspection data is monitored using Statistical Process Control (SPC). SPC is a tool aimed at controlling and, hopefully, improving a process

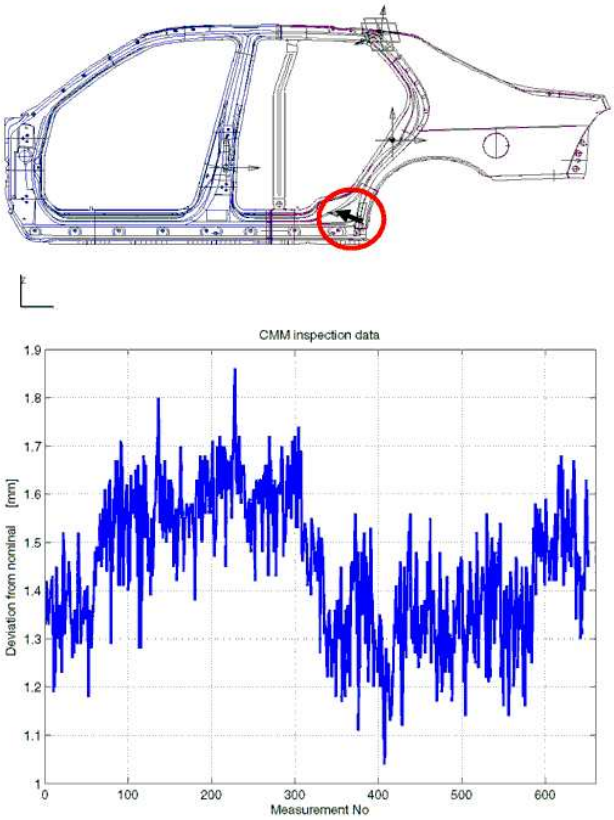

Figure 1.7: *In the top of the figure the inspection point in question is encircled. Below, CMM data for this point. There are 217 samples, where each sample consists of three objects.*

through statistical analysis of inspection data. More about SPC can be read in Chapter 2.

1.4 Finding root causes

Sampling, measuring machines and SPC-methods are tools for detecting deviations and variations in a process. When a variation is detected, it is essential to identify the cause of the problem. Sometimes the cause is obvious. Sometimes finding the variation source is a very demanding and time-consuming work, since variation propagates in a complex way during assembly. Today, much of this work is based on experience and a good process-knowledge. However, some problems may still be difficult to solve; an illustration of this was given in Figure 1.4. Further, merely depending on a small number of experienced problem-solvers makes the organization vulnerable. The methods for root cause analysis (RCA) presented in the following chapters are a set of tools for identifying fixture related causes of variations. Very concisely, the first step in RCA is to find a relation between variations in the P-frames of the parts and the resulting variations in the inspection points of the final subassembly. Using this relation, variation in inspection data can be translated to variation in one or more of the locators.

In Figure 1.8 a future RCA working procedure at Saab is outlined. If the SPC chart indicates increased variation and the reason of this phenomenon is unknown, then the user orders a root cause analysis. The sensitivity matrix A, containing product and process knowledge, is a part of the analysis and is calculated from a virtual model of the assembly. The RCA can be based on inline data or CMM data. The inline data is quickly available and is usually the first choice. However, since only a reduced number of points are measured here, that may not give enough information for a RCA. In that case, a RCA based on CMM data is performed. This gives usually a satisfactory result that is the base of an action to reduce the variation in the process. In some cases the method for RCA requires a modification to suit the current case, like excluding inspection points that not reflect the fixture related errors. RCA will be described more thoroughly in Chapter 3.

1.5 Geometrical variation

Geometrical variation in assembled products is a general problem in automotive industry. In this section, the causes and effects of geometrical variation, as well as different possibilities to reduce and handle the effects in different stages of the process development cycle, will be discussed.

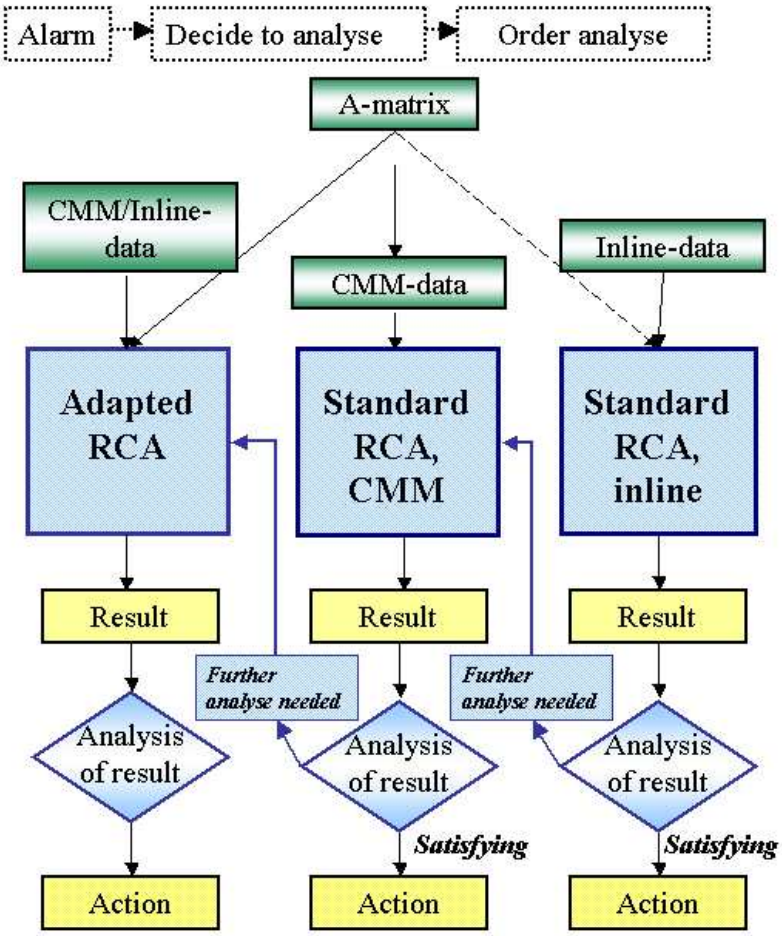

Figure 1.8: *An outline of a possible working procedure at Saab for RCA.*

1.5.1 Causes and effects of geometrical variation

Geometrical variation in parts and assembly process results in variation in size, shape and position of subassemblies or final products. This may

lead to difficulties in assembling parts or products not fulfilling functional and esthetical requirements. In Figure 1.9 examples of areas that can be af-

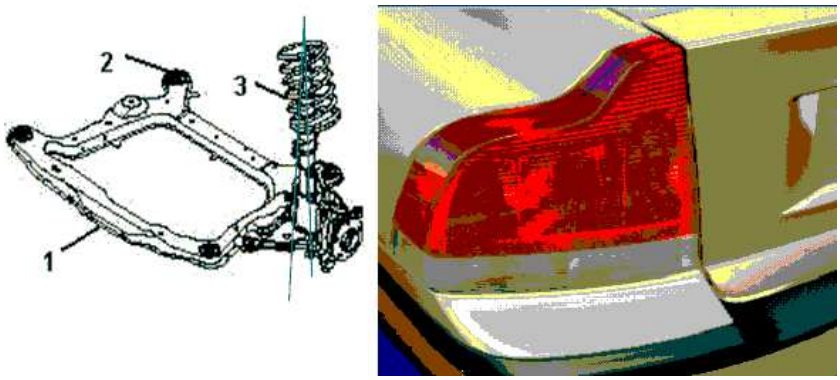

Figure 1.9: *Geometrical variation can cause problems with cumber/caster-angles and poor fit.*

fected by geometrical variation are shown. To the left, variation in camber- and caster angles can affect the driving characteristics of the car. To the right, variation during assembly can give rise to non-nominal flush between for example lamp and applica. Problems caused by geometrical variation are often discovered quite late in the product development cycle, maybe during pre-production or even when the product and the process are prepared for full-scale production. A correction of the problem at this phase is often very costly and time-consuming.

There are usually a number of different sources of geometrical variation in key characteristics of the assembled product; variation in parts and assembly process is thought two major contributors, see Figure 1.10.

Geometrical variation is controlled by locating schemes and by tolerances. The locating schemes describe how parts are positioned during assembly and was described in the Section 1.2. The tolerances are allocated with respect to assembly sensitivity, process variation and cost.

1.5.2 How to minimize the effects of geometrical variation

The principles of this section are based on the results within the 3DTM project.

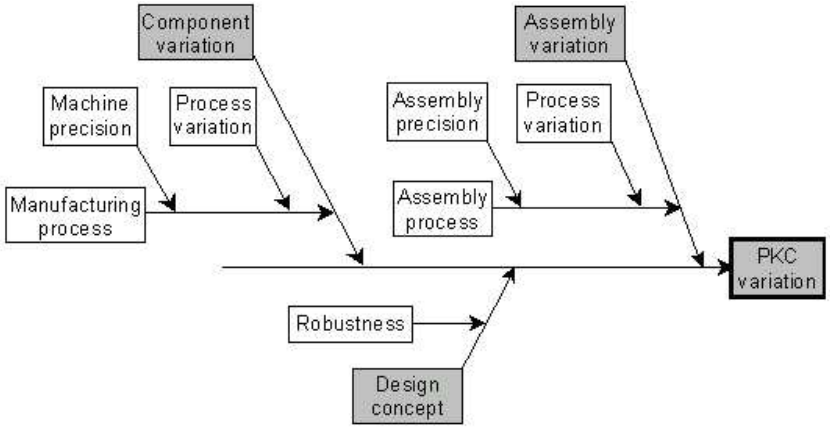

Figure 1.10: *Major sources of variation in a Product Key Characteristic (PKC) of an assembled product, Carlson et al. (7)*

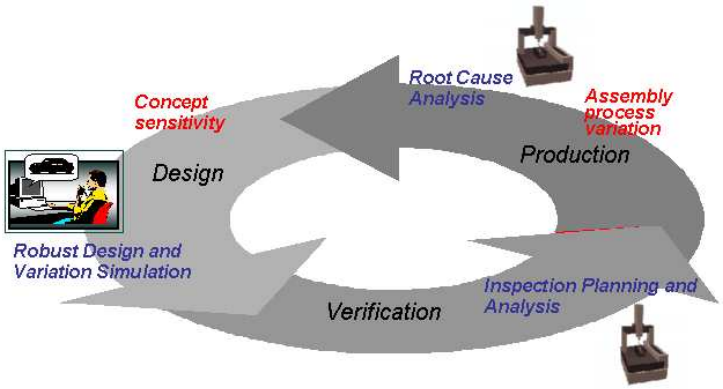

Figure 1.11: *Geometrical variation and tolerance management in a development cycle of products, Carlson et al.(7).*

The development cycle can be divided into three main parts; the design phase, the verification phase and finally the full production phase, see Figure 1.11.

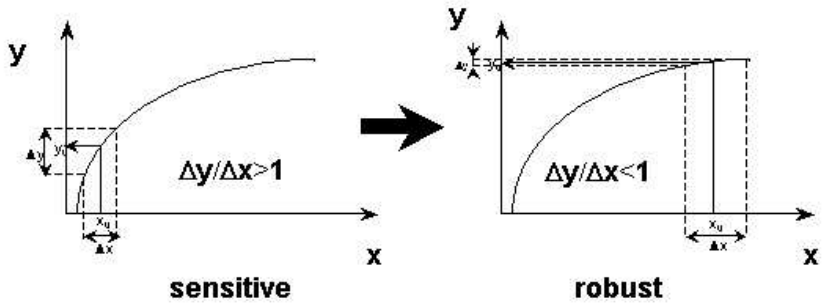

Figure 1.12: *A robust design is characterized by the fact that its important output characteristics are insensitive to disturbance, i.e. variation in input parameters, Söderberg and Lindkvist (31)*

During the first phase, the design phase, it is important to find a robust design concept. A robust design suppresses incoming variation, i.e. the design makes the variation in the output less than the variation in the incoming parts, see Figure 1.12 for an illustration. In order to find a satisfying design concept, it is usually necessary to test different concepts and evaluate their robustness and characteristics. One way of doing this is using prototypes and full-scale models. However, this is expensive and time-consuming. Further, it is not possible to try as many concepts as may be desirable. Using a virtual model is a much more effective way of testing different concepts. However, there are high demands on the software. It must of course be user friendly and offer suitable analysis tools. Further, it is interesting to examine the difference in perception of virtual and physical models. Wickman and Söderberg (37) showed that usually the physical model is experienced as better than an equivalent virtual model, analysing physical requirements.

Within the 3DTM research project, a software called *Robust Design and Tolerancing* (RD&T) is developed. This software offers different types of analysis of an assembly, like

- Stability analysis: Evaluates geometrical robustness and degree of coupling.
- Variation analysis: Statistical analysis of variation in critical dimensions.
- Contribution analysis: Ranking of variation contributors.

The analyses show how chosen key characteristics are affected by different tolerances and perturbations in the locating scheme. These facilitate the design of a robust concept and the allocation of tolerances with respect to assembly sensitivity, process variation and cost. Using the contribution analysis it is also possible to get a ranking list of the tolerances contribution to the variation in a chosen point. This ranking list is helpful if the variation in a specific point must be reduced. These analyses are illustrated on the assembly shown in Figure 1.13. It is a rear wheelhouse that is as-

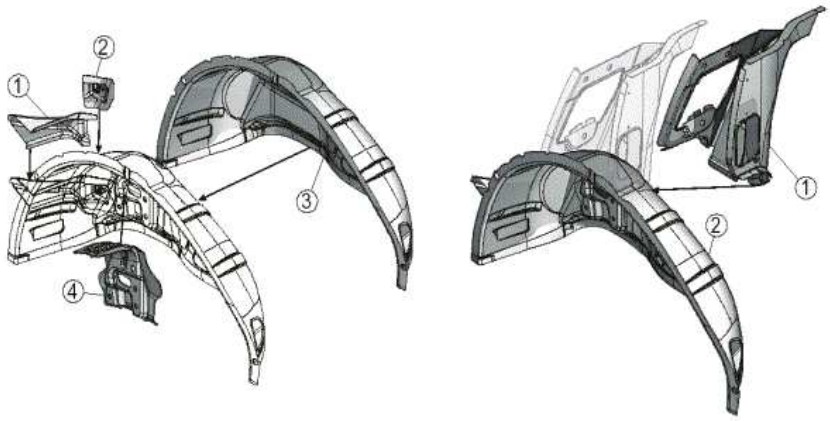

Figure 1.13: *The rear wheelhouse consists of five parts. The parts are assembled in two stages.*

sembled in two stages. In the first station three reinforcements (labelled 1,2 and 4) are put together with the wheelhouse panel (labelled 3). In the next step, this subassembly is moved to another station. In this station the subassembly is positioned using the same locators that were used to hold the panel in the first station. The support for the parcel shelf (labelled 1 in the right part of the figure) is put together with the subassembly, and finally the complete assembly is measured in an inspection station. During inspection the assembly is again positioned using the locators of the

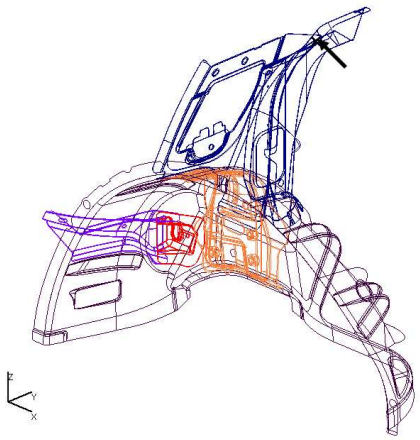

Figure 1.14: *The position of the inspection point labelled "Mea14" is illustrated by an arrow.*

wheelhouse panel. This assembly is analysed using the different kinds of analysis available in RD&T. For the variation and contribution analyses an inspection point called "Mea14", located on the upper part of the parcel shelf support, is utilized. The exact position of "Mea14" is illustrated in Figure 1.14.

The stability analysis for the wheelhouse is shown in Figure 1.15. The stability matrixes reflect the robustness and the degree of geometrical coupling in the assembly. The matrix elements relate the input columns, the P-frames, to the output parameters, the parts. A high value of a matrix element indicates that the input P-frame has a high influence on the part position. The value shown in the matrix is the root sum square (RSS) value of the six individual points of the P-Frame. For stability analysis, the only information needed is the nominal position of locators for parts and fixtures. Therefore, this analysis is a usable tool in the early design phase.

On the last row of the stability matrix shown in Figure 1.15, the degree of robustness for the parcel shelf support is shown. The measured position of this part is depending on the positioning of the wheelhouse in the inspection station, on the positioning of the subassembly from station one in

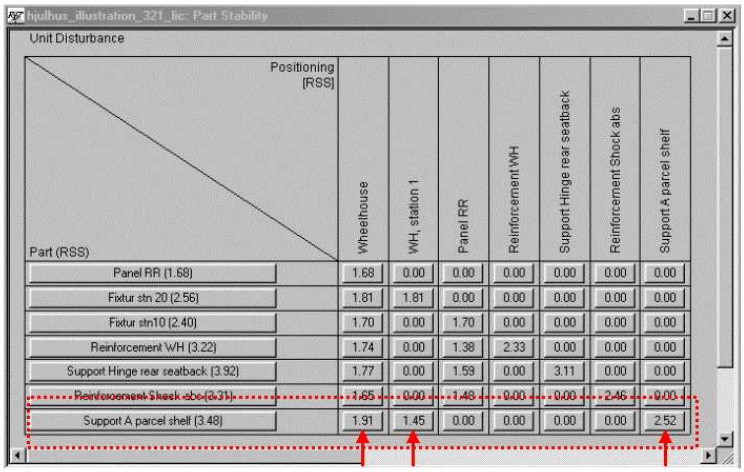

Figure 1.15: *Stability analysis, rear wheelhouse.*

stage two when the parcel shelf support is assembled, and of course, on the positioning frame for the part itself.

A variation analysis of the wheelhouse assembly is shown in Figure 1.16. The variation analysis uses Monte Carlo simulation technique to analyse variation in specified points. Tolerances for contacts between parts and fixtures are chosen by the user. Figure 1.16 shows the simulation results for the inspection point "Mea14", which position was illustrated in Figure 1.14. The specification limits for this inspection point are set to 0 ± 1.25 mm. The variation analysis shows the mean value, standard deviation, capability index et cetera for the simulations. These results give an indication on how well tolerance demands can be satisfied. In this case there are high capability indices; $C_p = C_{pk} = 2.89$, and these tolerances will most likely not cause problems in production.

The result of the contribution analysis of the wheelhouse is shown in Figure 1.17. The same inspection point as in the variation analysis is considered. The contribution analysis presents a ranked list of all points and tolerances contributing to measure variation. This analysis may be used in the work of optimising the selection of tolerances, and for trouble shouting during production. In this case, the locator A2 on the panel is the major

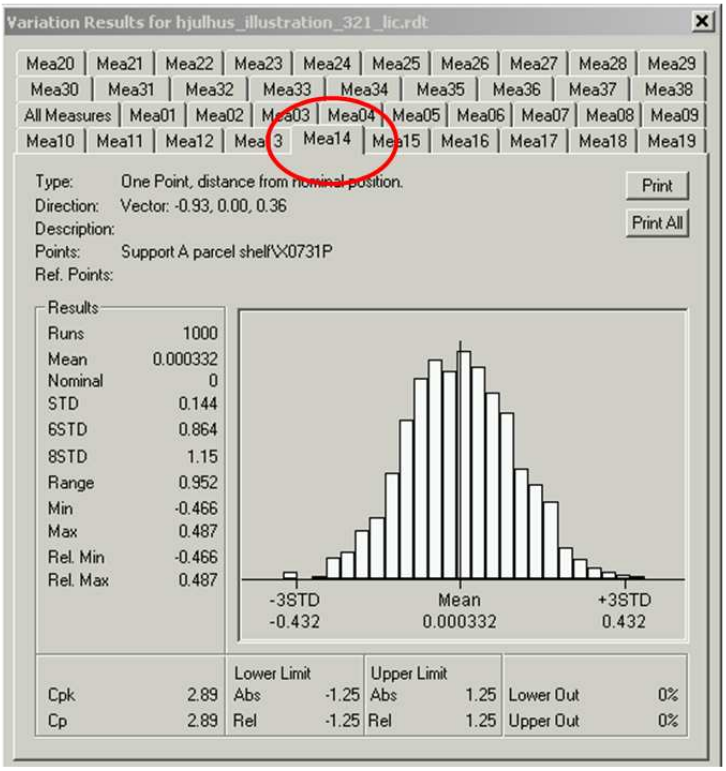

Figure 1.16: *Variation analysis, rear wheelhouse.*

contributor, since this locator give rise to 20.5% of the variation in this inspection point.

RD&T and the different analyses available in the program are further described by Lindkvist and Söderberg (24) and Söderberg and Lindkvist (30).

When a satisfactory design concept is chosen, the verification phase starts, see Figure 1.11 on page 13. During this stage, the design concept will be confirmed through tests and different pre-production series. It is important to keep this phase as short as possible. Today new car models are launched frequently and a requirement for doing this is short verification phases. Important activities at this stage are inspection planning and

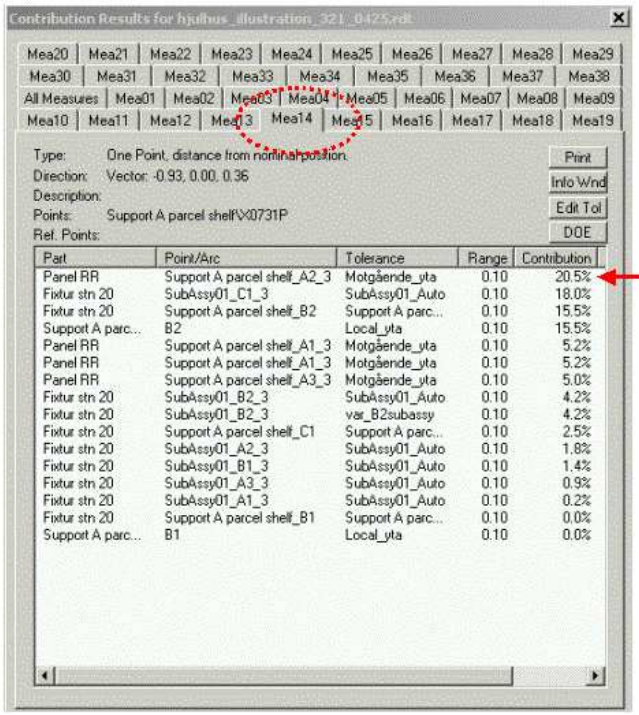

Figure 1.17: *Contribution analysis, rear wheelhouse.*

measurement machine programming.

In the last phase in Figure 1.11 the production starts and during this phase it is important to monitor and control the process in order to detect offsets and variations, which may result in non-conforming products and big costs. A suggestion of a system for detecting such problems is given in Chapter 2. Of course, it is also necessary to identify the root cause of a detected problem. Methods for finding root causes of geometrical variation will be considered in Chapter 3.

Chapter 2

A System for Acceptance Quality Control

2.1 Introduction

Companies with complex production systems and products have often problems with process variation affecting the products key characteristics. Traditionally, a control chart is used to detect if the process is in statistical control and therefore should be left alone, or if there are reasons for process adjustments. However, some of this variation is very difficult to eliminate at a reasonable cost. In this chapter we propose a quality system that allows for trends in the processes as long as the produced items are within specifications. Industrial data are used to illustrate the different charting methods.

2.1.1 Outline

The outline of the chapter is as follows. A background to the topics discussed is given in Section 2.1.2. In Section 2.2 problems related to a system for quality control are concidered. Methods proposed to solve those problems for different types of data are described in Section 2.3. This is followed by a discussion about when to use an acceptance control chart instead of a traditional chart in Section 2.4. Finally, the conclusions can be found in Section 2.5. In the Appendix an overview of some frequently used control charts and capability indices are given.

2.1.2 Background

During the car manufacturing process, many parts are joined together. The geometries of the resulting subassemblies are controlled by measuring deviations from nominal values in a set of inspection points. Often, many inspection points on each subassembly are utilized to give a good understanding of the assembly process. The inspection data is grouped or ungrouped.

The demands on the quality system are that the charts will be easy to interpret and the same kind of chart will be used for all inspection points belonging to the same category (grouped or ungrouped data). Further, the estimates required will be calculated in the same way for all data belonging to the same category. This is necessary since there is a great number of inspection points to which the charts will be applied and it is far too time consuming to find special solutions for every point. There are also many different users of the charts, and not all users are aware of the characteristics of different estimates and charting methods.

In a typical process, there are trends and cycles that result in variation in the mean value. Some of this variation is very difficult to eliminate at a reasonable cost. This variation may correspond to seasonal variations in temperature, different workers, different batches of raw material and also some unknown factors. For each inspection point there is an upper specification limit (USL) and a lower specification limit (LSL). The tolerance limits are product rejection/adjustment limits, so it is vital that the produced items are within the specified limits. As long as that is fulfilled, the group means may be allowed to vary over time. Of course, it is always good to keep the process in control and to improve the process. This is illustrated by Taguchi's loss function, see Figure 2.1. Taguchi (33) claims that every deviation from the target represents a loss, and the size of the loss is increasing with the size of the deviation. However, if the resources are limited, the first priority is to produce items within the specification limits. That means that under these circumstances, an acceptance chart may be preferable over a usual control chart.

So, the traditional control charts might not always be the best choice when the resources are limited. This issue, with the belonging questions about what acceptance charts to use, is partially discussed by Woodall (38). One of the methods discussed is pre-control. Pre-control is based on the tolerance limits and means that the range of the tolerance limits is divided into four parts of equal length. The middle two parts constitute the green zone, the outer two parts are the yellow zone and the area outside the tol-

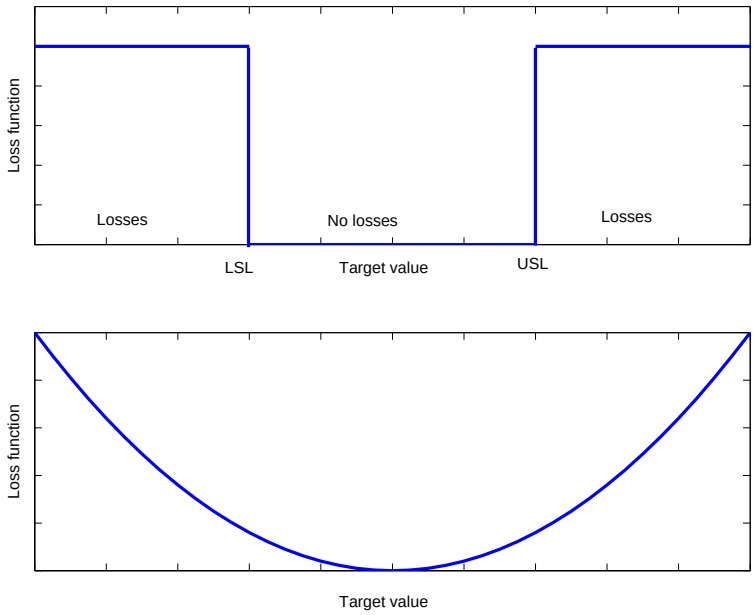

Figure 2.1: *Above: A usual way of thinking. All items within specification are considered equal. Below: Taguchi's loss function.*

erance limits is called the red zone. The process is allowed to operate as long as the inspection data do not fall into the red zone or into the yellow zone too often. There is a range of sampling and decision rules to ensure this. Woodall (38) among others, points out that the pre-control believers promote the idea with a lot of exaggeration. However, a pre-control chart gives no information about the statistical control of a process.

There are other methods beside pre-control that are based on the tolerance limits and can be used for controlling the mean value of a process. These so called acceptance control charts may be used when the process has a high capability. Consider a normally distributed variable with expected value μ and variance σ^2. The idea is to allow the mean value, $\bar{x}$, to vary over an interval $(\mu_{lower}, \mu_{upper})$, such as the fraction non-conforming produced items is at most δ, see Montgomery (25). Further, it is desirable to have a probability α of a type I error, i.e. a false alarm. This is achieved by using an upper control limit

$$UCL = USL - (Z_\delta - \frac{Z_\alpha}{\sqrt{n}})\sigma,$$

and a lower control limit

$$LCL = LSL + (Z_\delta - \frac{Z_\alpha}{\sqrt{n}})\sigma.$$

A quantity $Z_p\sigma$ is a value such that $p = 1 - \Phi(Z_p)$, where $\Phi(x)$ is the value of the standard normal cumulative distribution at the point x. By using these limits the chart gives an alarm when the mean value is so close to a tolerance limit that the expected fraction non-conforming exceeds δ. The

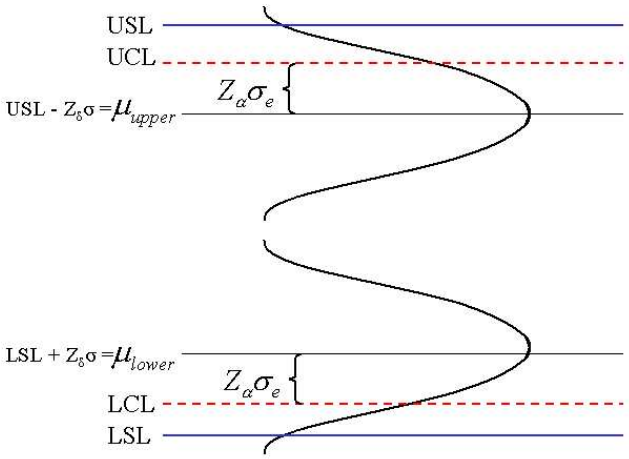

Figure 2.2: *Positions of control and specification limits in an acceptance chart for controlling mean value of a process, related to* μ_{upper} *and* μ_{lower}*, the largest respective smallest permissible value of* μ*. The notation* $\sigma_e = \sigma/\sqrt{n}$ *is used.*

positions of the UCL and USL are illustrated in Figure 2.2.

Chang and Gan (9) use the same method as Montgomery, but express the fraction non-conforming as a capability value. They test the method on data from an integrated circuit assembly and calculate the power function for a one-sided acceptance control chart.

Considering ungrouped data, an EWMA-chart is a better alternative for controlling the mean value than the $\bar{x}$-chart, since the EWMA-chart is creating a group-structure in data, making the chart more sensitive to

small deviations. A brief overview of the EWMA-chart is given in the Appendix. An acceptance control chart based on the usual EWMA-chart is considered by Holmes and Mergan (15). The principles are the same as for the acceptance chart for $\bar{x}$. Using the same notations as before, the process mean value, $\bar{x}$, is allowed to vary between μ_{lower} and μ_{upper}, such as the fraction non-conforming produced items is at most δ. If the probability of type I error is α, the control limits are given by

$$UCL = USL - Z_\delta \sigma + Z_\alpha \sigma_m,$$

and

$$LCL = LSL + Z_\delta \sigma - Z_\alpha \sigma_m.$$

The quantity σ_m is the standard deviation of m, the weighted exponentially moving average, and can be expressed as

$$\sigma_m = \sqrt{\frac{p}{2-p}}\sigma,$$

where σ is the standard deviation of the originally variables and p is the amount of weight put to the current value in the EWMA-chart. Holmes and Mergan (15) illustrate the method using simulated data.

2.2 Problem

This section describes problems related to quality control and gives motives for a new system for acceptance control, based on as well traditional control charts as the acceptance control charts introduced in the previous section.

The manufacturing process is often quite complex with many sources of variations. Since many of the causes of variation depend on long-term, but recurring, external conditions, operators and other unknown factors the data contains trends, see Figure 2.3 for an example. Those trends must be taken into consideration when the quality control system is designed.

The terms within-group variation and between-group variation are used to describe different kinds of variation for grouped data. The within-group variation is the variation in each sample, while the between-group variation can be seen as a factor determining the locations of the group means. In Figure 2.4 the group means are plotted together with the individual observations. The sizes of the group ranges, illustrated for the first three samples

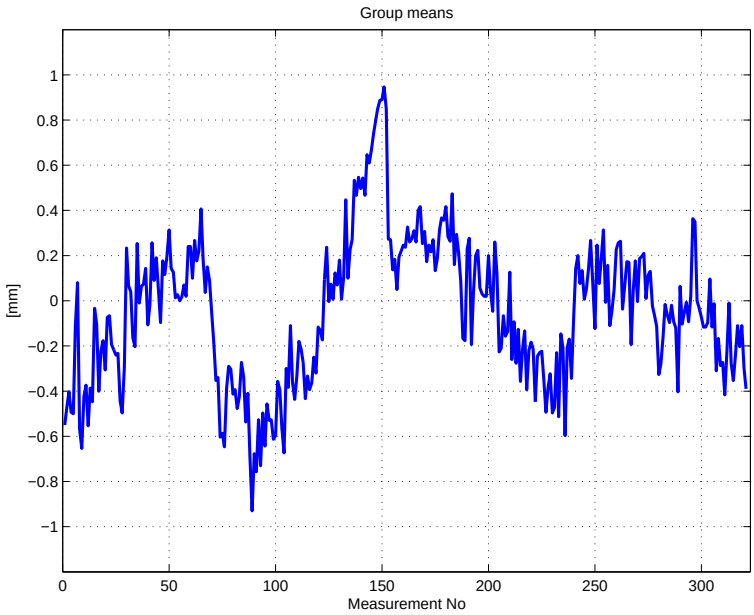

Figure 2.3: *The sample group means for a typical process. Deviation from nominal value are measured*

in the figure, are connected to the within-group variation. The group means differ though more than what can be expected due to within-group variation. Those are namely also affected by the between-group variation caused by external conditions, operators et cetera. If the data are ungrouped, the corresponding terms short-term variation and long-term variation are used.

Another problem is that the inspection data in the automotive industry are often of two different categories; ungrouped or grouped data. The ungrouped data originate from inline measurements. Every produced item is measured in the inline measurement machine as a step in the production. The grouped data consists of samples of n items each measured offline in coordinate measurement machines (CMM's).

The reason for using both inline- and offline-inspection is that the two approaches complement each other. The inline-measuring machine is fast enough to measure every produced item and it gives therefore a very good picture of the process. It is designed for detecting variations in the process quickly. The precision, i.e. the repeatability, in the inline measurement is

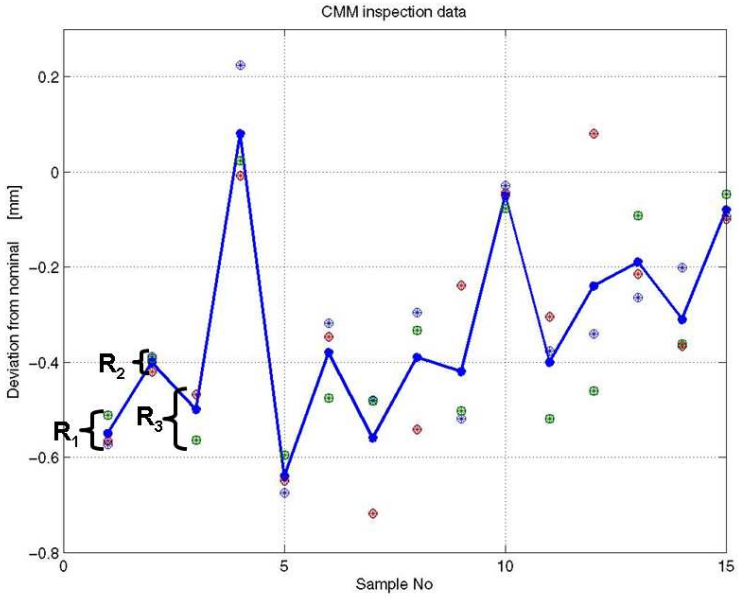

Figure 2.4: *The groupmeans are plotted together with the individual observations.*

good. There may though occur long-term variation in the measurement machine and the measured value may not be in agreement with the true value, i.e. the accuracy is not so good. Therefore, the inline measurement machine is best suited for controlling the short-term variation. The CMM on the other hand, has a very good accuracy. The precision of the CMM is also good. Since the CMM is used offline, there is also time to measure more inspection points on each item then during the inline-inspection.

At Saab Automobile AB, the sample size is $n = 3$, and the samples are usually taken once or twice a week. Each inspection point has an upper and a lower tolerance limit, and today these tolerances are the basis for the process control. The alarm limits for the mean value are set to 70% of the tolerance limits. The same method is used for the range; the range must not exceed 70% of the tolerance width. If these requirements are not met, there is an alarm. These alarms initiate fault localization and possibly a correction of the process.

There are many arguments against process control based on tolerance limits. Since the tolerances do not always reflect the characteristics of the process, problems may occur. In all kind of process control, there are two types of mistakes. The first one, the Type I error, is to take action when the process has not changed. The second one, called Type II error, is to not take action despite a change has occurred. The tolerance limits are set due to functional and design requirements and of course, also due to process performance. Despite this, the tolerance limits are not related to the mean and variance of the process in such a way that the probability of the different types of errors can be controlled. Nevertheless, the tolerance limits are a very important factor in a quality control system.

Consider a control chart based on the tolerance limits. If the capability of the process is low, the probability of type I error will be high. If an already centered process is adjusted due to these false alarms, the process will perform even worse and even more items outside tolerance will be produced. For a low capability process, a traditional control chart is the best chart in order to analyse and improve the process.

On the other hand, when the capability of the process controlled by using tolerance limits is high, the probability of type I is small and the probability of type II error is high. A type II error is though preferable to the type I error and might not be a major concern, as long as the process is capable and produces conforming products. Actually, it might be desirable to avoid alarms as long as the produced items are well within the specifications, in order to cut down the costs. One way of handle this is to use acceptance control charts, mentioned in the introduction. Such a chart allows trends and variation, provided the produced items are within specifications.

To summarize these thoughts, it would be desirable to have a system for quality control that consists of two different types of chart. Traditional control charts should be used to improve and control low capability processes. This kind of chart helps bringing the process in statistical control and can also be used as a tool for reducing trends and variations in the process. For a high capability process on the other hand, eliminations of these trends are not always economically justifiable. In those cases, an acceptance control chart is suitable, since it allows variation provided that the produced items are well within specifications.

2.3 Proposed methods

As mentioned, there are two different kinds of data, grouped and ungrouped measurements. In the grouped data the group structure is utilized for increasing the sensitivity of the chart. For ungrouped data some kind of artificial group structure is usually created. Therefore, different charting methods are used for these two categories of data. Further, charts for controlling the mean value can be of two types; a traditional $\bar{x}$-chart if the process has a low capability or an acceptance control chart if the process capability is high. In this section all those different types of charts are described. Range-charts for controlling the variation in the process are also discussed for the different types of data.

2.3.1 Grouped data

For control of the mean value of the process, there are two different alternatives, depending on the capability of the process. If the capability is low, it is important to improve the process and avoid Type II errors. In this case, a traditional control chart is used. If the capability is high, some trends may be allowed, provided the produced items are within the specification limits. In this case, some kind of an acceptance chart may be used.

Traditional control charts

This alternative is suitable for a process with low capability and is a tool for improving the process.

The grouped data available for estimating the parameters of the process consist of k samples of size n. In the examples, $n = 3$. Let x_{ij} be the j:th observation in the i:th sample for $i = 1, 2, ..., k$ and $j = 1, 2, ..., n$. For each group the sample group mean,

$$\bar{x}_i = \frac{1}{n} \sum_{j=1}^{n} x_{ij}$$

and the sample group variations

$$s_i^2 = \frac{1}{n-1} \sum_{j=1}^{n} (x_{ij} - \bar{x}_i)^2$$

are calculated. The within-group variation σ_w^2, is estimated by the mean of the group variances:

$$s_w^2 = \frac{1}{k} \sum_{i=1}^{k} s_i^2.$$

Further, the total sample mean $\bar{\bar{x}}$ and the sample variation of the group means, s_B^2, is determined in the following way:

$$\bar{\bar{x}} = \frac{1}{k}\sum_{i=1}^{k}\bar{x}_i$$

$$s_B^2 = \frac{1}{k-1}\sum_{k-1}^{k}(\bar{x}_i - \bar{\bar{x}})^2.$$

The estimated variation of the group means, s_B^2, will contain contributions from both within-group variation, σ_w^2, and between-group variation, σ_B^2, since

$$V(\bar{x}_i) = \sigma_B^2 + \sigma_w^2/n.$$

The process is controlled by a $\bar{x}$-chart and a range-chart. The control limits of the $\bar{x}$-chart are usually given by

$$CL = \bar{\bar{x}} \pm 3\frac{s_w}{\sqrt{n}}.$$

If it would be desirable to allow between group variation the following control limits can be used, Wetherill and Brown (36),

$$CL = \bar{\bar{x}} \pm 3s_B.$$

By using these control limits as well within-group variation as between-group variation are permitted. Using this kind of control limits allow for trends, but unlike the acceptance control charts, the specification limits are not taken into consideration. Therefore, this chart does not necessarily alarm, even if the trends cause the products to be out of specifications.

The estimates should be based on data representing a satisfying part of the process. It is necessary that the data is representative for the process and covers a period long enough to reflect the behaviour of the process.

If this procedure leads to control limits close to, or even outside, the tolerance limits the cause of this must be examined. There are two possible reasons; one is that the process is not centred in the tolerance band and the other is that the variation is too big compared to the tolerance width. If the problem is due to offset, the consequences of this offset must be examined. If the offset does not affect the product negatively, it will usually be accepted, and the tolerance limits will be updated. Otherwise, it must be corrected. If the problem is due to variation, actions to reduce this variation should be taken. Of course, this problem may have been caused by a

temporary deviation in the process and in such case it is not appropriate to include these data in the parameter estimation of the control chart limits.

It is also necessary to control the within-group variation for a sample. To do that a range-chart can be used. In the range-chart the group ranges are plotted. The upper control limit is given by

$$UCL = D_1 s_w$$

and the lower control limit, if such one is used, is given by

$$LCL = D_2 s_w.$$

The values of the constants D_1 and D_2 depend on n, the number of observations in each group, and can be found in for example Wetherill and Brown (36). When $n = 3$, $D_1 = 0.06$ and $D_2 = 5.06$. There is no relation between specification limits and the range of a group. Further, the ranges are not affected by trends or between-group variation.

Acceptance control chart for mean value

Another alternative for controlling the mean value is to use some kind of acceptance control chart, if the process has a high capability. The benefit is that alarms are avoided when the items produced are far enough from the specification limits. The alarm limits for an acceptance chart, described in the introduction, are based on the maximal fraction non-conforming units, δ, that can be tolerated. The fraction non-conforming corresponds to the process capability. In the automotive industry $C_p > 1.33$ is often used as a target. This corresponds, as the following calculations show, to a fraction non-conforming $\delta < 6.61 * 10^{-5}$ if the process is centred, i.e. $C_p = C_{pk}$, since

$$\frac{USL - \mu}{\sigma} = \frac{\mu - LSL}{\sigma} = 3 * 1.33$$

and

$$\begin{aligned} P\{non - conforming\} &= 1 - P\{LSL < X < USL\} = \\ &= 1 - \{\phi(\frac{USL - \mu}{\sigma}) - \phi(\frac{LSL - \mu}{\sigma})\} = \\ &= 1 - \{2\phi(3 * 1.33) - 1\} = 6.61 * 10^{-5}. \end{aligned}$$

This fraction of non-conforming items corresponds in a one-tailed distribution to $Z_\delta = 3.82$.

The control limits for an acceptance chart for the mean value, described in Section 2.1, are given by

$$UCL = USL - (Z_\delta - \frac{Z_\alpha}{\sqrt{n}})\sigma$$

and

$$LCL = LSL + (Z_\delta - \frac{Z_\alpha}{\sqrt{n}})\sigma.$$

The probability of Type I error is determined by α, and a usual choice is $\alpha = 0.0013$. This value corresponds to $Z_\alpha = 3$. The standard deviation σ is estimated by the within-group standard deviation, s_w. The within-group variation is used since the mean value is allowed to vary within an interval $(\mu_{lower}, \mu_{upper})$, such that when $\mu = \mu_{upper}$ or $\mu = \mu_{lower}$, the fraction non-conforming is δ. The position of μ is examined for each group and for the observations in a specific group the variance is given by σ_w^2. When using this chart, it is important that the variation σ_w^2 of the process is in control, this is examined by using a range-chart.

When an acceptance chart is used, there is no alarm if the process is out of control, as long as $\mu_{lower} < \mu < \mu_{upper}$. This is a way to reduce costs, since when μ belongs to this interval the probability of producing a non-conforming item is less then δ. However, if $\mu = \mu_{upper}$ or $\mu = \mu_{lower}$ the chart is designed to detect an increase or decrease of the process mean. Hence, an alarm is always the result of the process being out of control, on the other hand there is not an alarm every time the process is out of control. In other words, the probability of Type II error is big when the process mean is in the interval $(\mu_{lower}, \mu_{lower})$, because then it is not desirable with an alarm, since the fraction nonconforming units is very small. But when the fraction non-conforming units increase, i.e. the capability decreases, the probability of Type II error decreases. This is illustrated using a power function, see Figure 2.5. The power is defined as $1 - \beta$, where β is the probability of Type II error, i.e. the power is the probability of detecting a change in the process.

In Section 2.4 there are examples of as well traditional $\bar{x}$-chart as acceptance control charts.

2.3.2 Ungrouped data

The ungrouped data origin from an inline measurement machine, i.e. all produced items are measured. Just as with the grouped data, it is possible

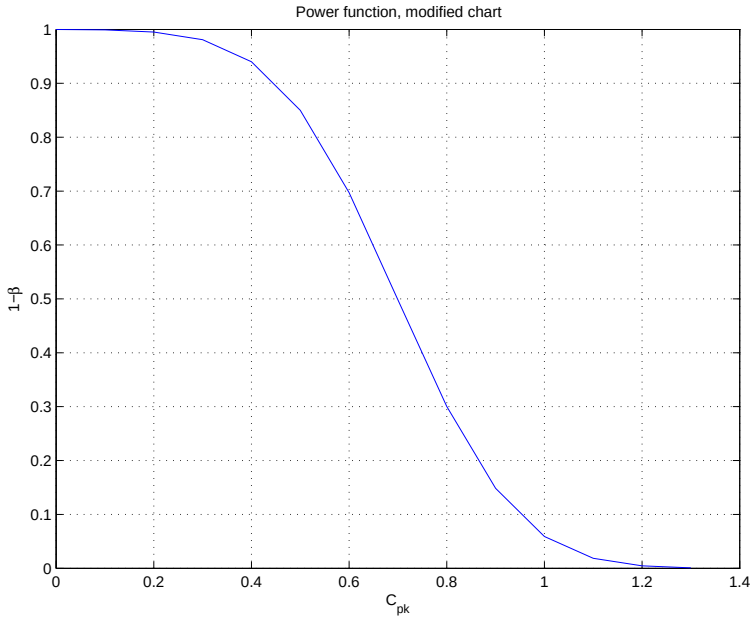

Figure 2.5: *Power function for an acceptance chart. When the capability is high, the probability of an alarm for a change in the process is small.*

to use traditional charts when the capability of the process is low and acceptance charts for controlling the mean value of high capability processes.

Data consist of a number of individual observations x_i. The estimates of necessary parameters are based on n observations.

Traditional control charts

To control the short-term variation in the process a moving-range chart is used. In the chart the range of a small number of consecutive measurements is plotted. The upper control limit is given by

$$UCL = D_3 * s.$$

The constant D_3 depends on the number of observations included in the moving range, and is tabulated by for example Wetherill and Brown (36). In order to control the short term variation, the moving range is usually based on two successive measurements. In that case, $D_3 = 4.65$. The sample standard deviation, s, is calculated from data using a moving range

method. This is done by calculating the moving ranges, R_j, for groups of size k, determine the mean range and then divide this number by a constant depending on the value of k, i.e.

$$s = \frac{\sum_j R_j}{\#ranges}/d_k,$$

where d_k is a constant depending on the size of the moving ranges and can be found in tables in for example Wetherill and Brown (36). Often, $k = 2$ is used. By using $k = 3$ slightly more variation than what could be expected in the moving ranges in the chart is permitted. If $k = 2$, then $d_k = 1.128$ and if $k = 3$, then $d_k = 1.683$.

It may also be desirable to use a chart for the mean value. However, the main potency of an inline measurement machine is to control the short-term variation in the process. If control of the mean value is required, then some kind of moving average chart should be used in order to enhance the sensitivity of the chart. An EWMA-chart is often a good choice, since compared to an ordinary moving average chart, more weights are paid to the last observations than to the earlier ones.

In an EWMA-chart

$$m_i = px_i + (1-p)m_{i-1}$$

is plotted. The constant p is the weight given to the most recent observation. A usual choice is $p = 0.4$. The control limits are given by

$$\bar{x} \pm A_1 s.$$

If $p = 0.4$ is used, then $A_1 = 1.545$ for ungrouped data. Values of A_1 for different values of p can be found in for example Wetherill and Brown (36). The sample standard deviation, s, is calculated by the moving range method. For the grouped data, we noticed that it sometimes may be desirable to allow between group variation. For the ungrouped data this corresponds to allowing-long term variation and the estimate of the standard deviation should in that case be based on all data. To calculate s^2 in that case, the following formula is used:

$$s^2 = \frac{1}{n-1}\sum_{i=1}^{n}(x_i - \bar{x})^2.$$

Acceptance chart using EWMA

Just as with the grouped data, it is possible to use traditional charts when the capability of the process is low and an acceptance chart for controlling

the mean value of a high capability process. The benefit is that alarms are avoided when the items produced are far enough from the specification limits. The alarm limits for an acceptance EWMA-chart, described in the introduction, are based on the maximal fraction non-conforming units, δ, that can be tolerated. Just as in the case with the $\bar{x}$-chart the maximal fraction non-conforming products, δ, is set to $6.33*10^{-5}$, which corresponds to capability of 1.33. The probability of false alarm, α, is 0.0013.

The control limits are given by

$$UCL = USL - Z_\delta \sigma + Z_\alpha \sigma_m,$$

and

$$LCL = LSL + Z_\delta \sigma - Z_\alpha \sigma_m,$$

where

$$\sigma_m = \sqrt{\frac{p}{2-p}}\sigma,$$

and σ is the standard deviation of the originally variables. The standard deviation σ is estimated by the moving range method described in the previous section. In Figure 2.6 are acceptance and traditional EWMA-charts plotted for an inspection point with high capability. The acceptance chart gives no alarms, since the plotted values are far enough from the specification limits. The traditional chart alarms, indicating that the process is out of control. However, in this case, the process being out of control does not result in an unacceptable fraction non-conforming items.

2.3.3 Multivariate data

To control several related inspection points at the same time it may be convenient to use a multivariate control chart. It is easier to only have one chart, instead of one for each point, and the multivariate chart takes the relationship between different inspection points into consideration. Further, by using a multivariate chart the total probability of a type I error is controlled. The disadvantage of a multivariate chart is that since it is used to control all the inspection points at the same time, it is sometimes difficult to identify the point or points that cause an alarm. Different kinds of multivariate control charts are discussed in Chapter 3.

The p-variate inspection data vector is supposed to follow a p-variate normal distribution $N(\mu, \mathbf{\Sigma})$.

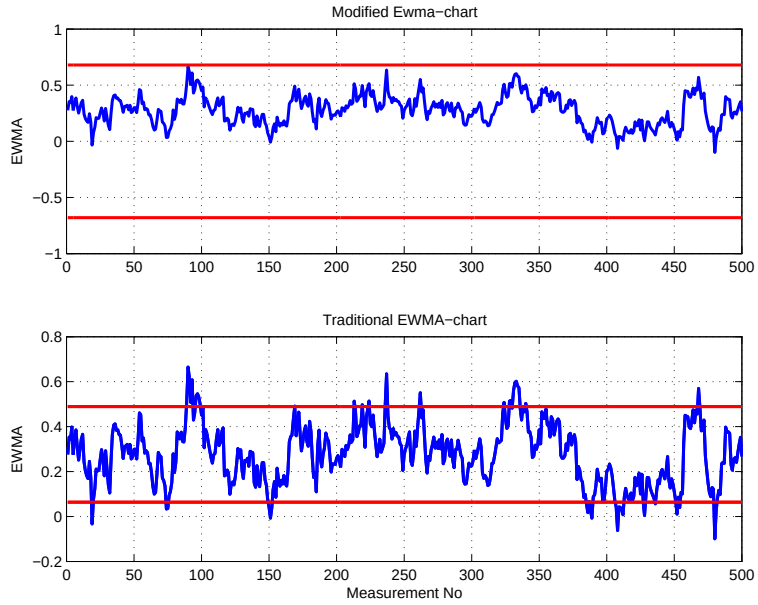

Figure 2.6: *EWMA-charts for a high capability process. The charts are based on measurements of deviation from nominal geometry at one inspection point.*

Multivariate capability indices

There are several different suggestions of multivariate capability indices. Three of these indices are compared by Wang et al. (35). These are a multivariate capability vector by Shahriari et al. (29), a multivariate capability index MC_{pm} by Taam et al. (32) and finally a multivariate capability index MC_p by Chen (10).

Naturally, all of these three indices have their advantages and disadvantages. Here, we have chosen to use the multivariate capability index MC_{pm} by Taam et al. (32). The index is defined as the ratio between the volume of R_1, the modified tolerance region, and the volume of R_2, the scaled 99.73 percent process region,

$$MC_{pm} = \frac{vol.(R_1)}{vol.(R_2)}.$$

The modified tolerance region, R_1, is the largest ellipsoid centred at the process target and completely within the tolerance region. Since data is

normally distributed R_2 is also an ellipsoid. The capability index is estimated by

$$\hat{MC}_{pm} = \frac{\hat{C}_p}{\hat{D}},$$

where

$$\hat{C}_p = \frac{vol.\,(tolerance\ region)}{vol.\,(estimated\ 99.73\%\ process\ region)} = \frac{vol.\,(tolerance\ region)}{|\mathbf{S}|^{1/2}(\pi K)^{p/2}(\Gamma(p/2)+1)^{-1}},$$

where K is the 99.73% percent quartile of a χ^2 distribution. The denominator $\hat{D}$ is given by

$$\hat{D} = \left(1 + \frac{n}{n-1}(\bar{\mathbf{X}} - \mu_0)^T \mathbf{S}^{-1}(\bar{\mathbf{X}} - \mu_0)\right)^{1/2},$$

The quantity $1/\hat{D}$ takes values between zero and one and measures the deviation from target. The closer $1/\hat{D}$ is to one, the closer is the processes to their targets. If the mean vector equals the target vector μ_0, $1/\hat{D}$ equals 1 and accordingly $\hat{MC}_{pm} = \hat{C}_p$. The quantity $\hat{C}_p$ is interpreted just like the univariate process capability, i.e. a value $\hat{C}_p = 1$ implies that 99.73% of the produced items are within the specification limits.

Multivariate acceptance control chart

The idea of a multivariate acceptance chart is analogous to the univariate acceptance chart. The starting point is to decide an allowable region for the mean vector of the p points, given an upper limit for the fraction nonconforming produced items. Thereafter, this process area is transferred into an allowable region for the mean value vector, given a type I probability α. The tolerance region is usually formed as a hypercube, at least when the specification settings are independent. This region must in some way be transformed into the same shape as the process region, which is an ellipsoid so the regions can be compared to each other. In the multivariate capability index by Taam et al. (32) the tolerance region is transformed to the largest ellipsoid completely within the tolerance region and centered at the process target. Using this procedure as a starting point, it should probably be possible to construct a multivariate acceptance control chart. This area is though subject to future research.

2.4 When to use an acceptance control chart?

A usual $\bar{x}$-chart gives with a high probability an alarm when the process mean changes. If there is no alarm, the mean value is stable and the process is in statistical control. An acceptance chart gives with high probability an alarm if the process is out of control and the mean value is to close to the tolerance limits. Another way of saying this would be to define a group capability index, $C_{pk}^{i} = \frac{min\{USL-\bar{x}_i, \bar{x}_i-LSL\}}{3\sigma}$ $\quad i = 1...k$, for every group. Then the acceptance chart gives alarm when the group capability index is too low. It is important to note that the group capability index says nothing about the future process performance, since the mean is allowed to vary.

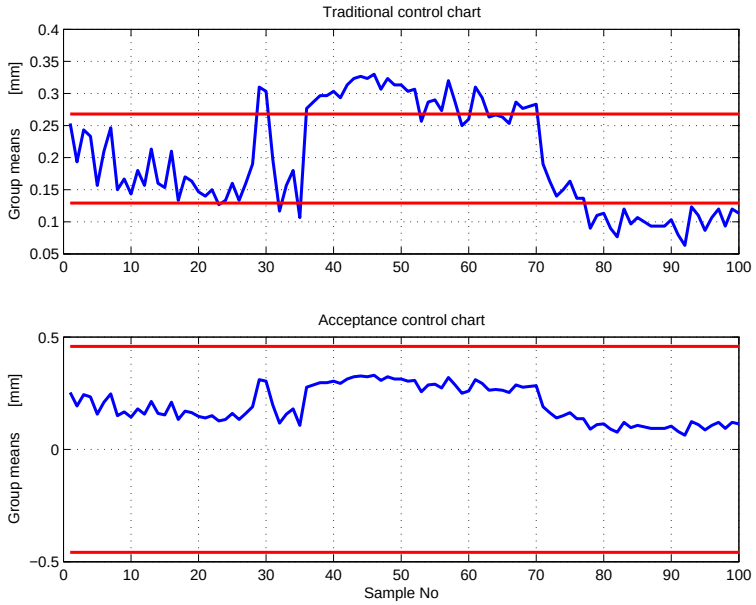

Figure 2.7: *Above: A traditional control chart for the mean value. Below: An acceptance control chart for the same data. The specification limits are* $\pm$ *0.5 mm.*

In Figure 2.7 an example of control charts for mean value of a high capability process is shown. The upper plot is based on the traditional methods, while the lower one is an acceptance control chart. The acceptance chart gives no alarms since the process is far from the specification limits. The upper chart indicates that the process is out of control. In this case, the process being out of control is not regarded as important, since the process

still produces items well within specifications, and the acceptance control chart is the preferable chart here.

In Figure 2.8 the circumstances are reversed. In this case the process has a low capability, and therefore the traditional chart is preferable. In the upper plot, the traditional chart indicates that the process is out of control. The reasons of this should be examined. Since the capability is low, the acceptance control chart in the lower part of the figure is not suitable.

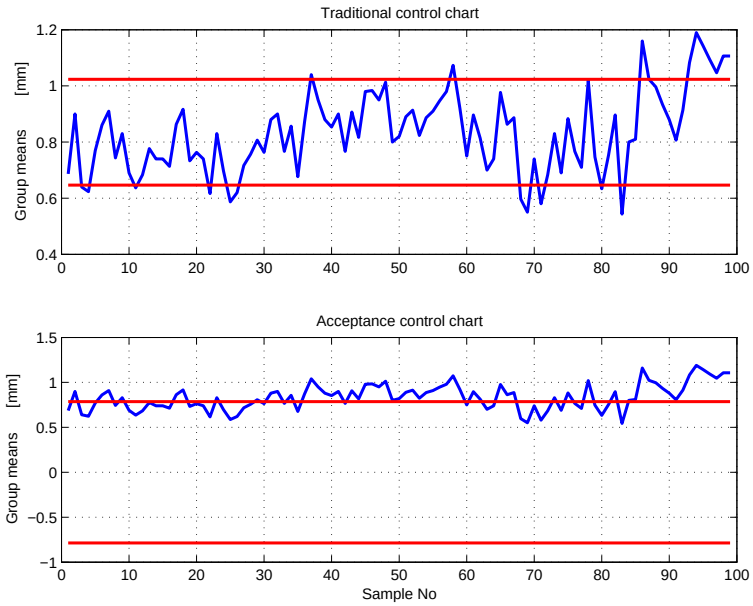

Figure 2.8: *Top: Traditional control chart for an inspection points with* $C_p = 2.76$ *and* $C_{pk} = 0.20$ *The specification limits for this point are* $\pm$ *0.9 mm. Below an acceptance control chart for the same data.*

The question is when to use traditional charts and when to use acceptance charts. At some point the control limit for a usual control chart and the control limit for an acceptance control chart coincide. This point can be expressed as a certain value of the capability of the process. The value

is determined assuming $min(USL-\mu, \mu-LSL) = USL-\mu$;

$$\begin{aligned} UCL_{acceptance} &= UCL_{\bar{x}} \\ USL-(Z_\delta - \frac{Z_\alpha}{\sqrt{n}})\sigma &= \mu + 3\frac{\sigma}{\sqrt{n}} \\ \frac{USL-\mu}{\sigma} &= \frac{3}{\sqrt{n}} + Z_\delta - \frac{Z_\alpha}{\sqrt{n}} \\ C_{pk} &= \frac{1}{\sqrt{n}} + \frac{Z_\delta}{3} - \frac{Z_\alpha}{3\sqrt{n}}. \end{aligned}$$

Using $n = 3$, $Z_\delta = 3.82$ and $Z_\alpha = 3$ this gives $C_{pk} = 1.27$. If the value of the adjusted capability index is below this value a usual $\bar{x}$-chart should be used. Otherwise, an acceptance chart is preferable.

It would also be possible to combine these two kinds of charts if the capability index $C_p > 1.27$ and the adjusted capability index $C_{pk} < 1.27$, by using a modified lower control limit and a usual upper control limit if $min(USL-\mu, \mu-LSL) = USL-\mu$ and vice versa.

2.5 Conclusions

In a typical process in automotive industry, there are trends and cycles causing variation in the mean values. Some of this variation is very difficult to eliminate to a reasonable cost. For each inspection point there are an upper specification limit (USL) and a lower specification limit (LSL), and sometimes it may be desirable to allow the variation in mean value as long as those specifications are fulfilled. The specifications can be fulfilled, despite the variation, if the process has a high capability. A low capability process on the other hand, must be improved, to avoid products out of specifications.

An overview of the different charting methods is given in Figure 2.9. Here the relation between what kind of data, process capability and what charts to use for controlling mean and variance of process are illustrated. The different methods were described and the question about when to use an acceptance chart instead of a traditional chart was also discussed.

If resources are unlimited, the ideal is perhaps to use some kind of traditional chart in order to analyse and improve the process. Unfortunately, this is not often the case, and therefore the system for quality control described in this chapter may be a way to improve processes to a level where

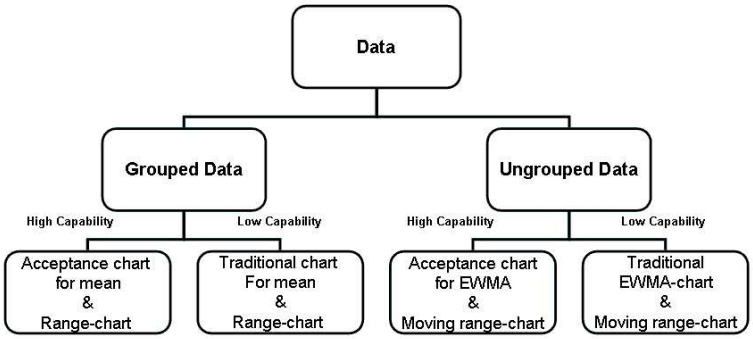

Figure 2.9: *An illustration of the different charting-alternatives.*

the items produced are within specifications, and to control that this level then is remained.

2.6 Appendix - Frequently used control charts and process capability

A control chart consists of a statistic, which is plotted in the diagram for each measurement. If the statistic plots outside the calculated values called control limits, there are assignable causes and the process is considered to be out of control. This means that the process is believed to have changed. The probability that the statistic plots outside the limits, despite the process remains in control, and causes a false alarm is denoted α. A common choice is $\alpha = 1\%$ or $\alpha = 0.1\%$.

To control the mean value of a process an $\bar{x}$-chart can be used, Wetherill and Brown (36). This chart is of Shewhart-type and is probably one of the most frequently used control charts today. This method assumes that the distribution of the plotted data is approximately Normal and uses the fact that most of the dispersion is included within $\pm 3\sigma$ from the mean. The upper control limit (UCL) and the lower control limit (LCL) of the chart are given by

$$UCL = \mu + 3\sigma_e \text{ and } LCL = \mu - 3\sigma_e,$$

where σ_e is the standard deviation of the group mean, i.e. if the standard deviation within a group of size n is σ_w, then $\sigma_e = \sigma_w/\sqrt{n}$. The expected value, μ, can be estimated by the mean $\bar{x}$.

Other methods used to control the mean value of a process are cumulative sum procedures (CUSUM) and exponentially weighted moving average (EWMA) charts. These procedures are especially useful to detect small shifts. In a CUSUM chart the cumulative sum, S_n, of the observations $x_1, x_2, ...$ is plotted, i.e.

$$S_n = S_{n-1} + (x_n - T),$$

where $S_0 = 0$ and T is a target value, often the mean is used as target. In the CUSUM chart a so-called truncated V-mask is generally used. An out of control signal is given when the arms of the mask cross the previous trace of CUSUM values.

The EWMA chart is basically formed by determination of a new moving-average at each sampling point by calculating a weighted average of the new value and the previous moving-average. The moving-average, m_i, is calculated using the formula

$$m_i = p\bar{x}_i + (1-p)m_{i-1}$$

where p is the amount of weight put on the current value. In an EWMA chart only action limits are used, and they are placed at $\mu \pm A_1\hat{\sigma}_e$, where A_1 is a tabulated value, depending on the group size.

The dispersion of a process can be controlled by using a s- or r-chart. The procedure is similar to the construction of a $\bar{x}$-chart. The standard deviation (or range) of each group is plotted and the control limits in this case are given by σ_w times a constant, see for example Wetherill and Brown (36).

The capability index of a process is reflecting the process's ability to produce items within the specification limits. The capability index, C_p is a comparison between the specification width and the width of the distribution. For a normal distribution 99.7% of the distribution is covered by 6σ and the process capability index is defined by

$$C_p = \frac{USL - LSL}{6\sigma}$$

Usually, $C_p > 1.33$ is recommended. A high capability process may still produce many non-conforming items if the mean is not appropriately centred. Therefore, another capability index sometimes called the adjusted capability index, C_{pk}, is defined,

$$C_{pk} = \frac{min\{USL - \mu, \mu - LSL\}}{3\sigma}$$

The definitions of the indices above are both based on a normal distribution assumption. Further, the process must be in control. Otherwise, the indices cannot be used as a prediction of the process performance. The indices can be calculated no matter what distribution the data have. However, if the indices will be used to predict the process performance it is crucial that the process is in control, otherwise the only information given is what the process performs at the moment when the data is collected.

Chapter 3

Multivariate Quality Control and Diagnosis

3.1 Introduction

In the auto body assembly process, fixtures are used to position parts during assembly and inspection. Geometrical variation in parts and in the assembly process results in variation in size, shape and position of the final product. This may lead to difficulties in assembling parts or products not fulfilling functional and esthetical requirements. Geometrical variation is controlled by locating schemes and tolerances. The locating schemes describe how parts are positioned during assembly. The tolerances are ideally allocated with respect to assembly sensitivity, process variation and cost.

Parts and subassemblies are measured many times during the manufacturing process in order to detect offsets and variations as soon as possible. In order to use data in an optimal way, statistical process control (SPC) may be used. It is a statistical analysis of inspection data aiming at controlling and, hopefully, improving the process. There is also a multivariate equivalence of SPC, the namely the MSPC suited for simultaneous analyse of data from several inspection points.

If an offset or variation is detected, it is of course desirable to find its root cause. For example bad raw materials, worn out machines or fixture faults can cause variation. But a major part of all root causes are due to fixture faults, according to an investigation performed by Ceglarek and Shi (8). In this chapter, methods for MSPC and methods for diagnosing variation in fixtures by using process knowledge and inspection data are

considered.

There are many different methods used in multivariate quality control. The purpose of this chapter is to illustrate and compare some of these methods by applying them to given data sets, collected from industrial case studies. The procedures for quality control are then put together with methods for fixture fault diagnosis. Different methods to diagnose the fixture or fixtures causing the error are illustrated using the same data sets.

3.1.1 Outline

This chapter is outlined as follows. In Section 3.2 the two case studies are presented. The methods described in subsequent sections will be applied to the data from these case studies.

In Section 3.3 different kinds of multivariate control charts are considered. Two special methods, aimed for detecting fixture related faults are also illustrated. For each type of chart the theory of the chart is described and thereafter the chart is tested on data from the case studies.

When a process is found to be out of control, it is obviously of main importance to find the root cause of the erroneously state. This topic is discussed in Section 3.4. The methods are demonstrated in the same way as in Section 3.3; the description of each method is followed by a test on data from the case studies.

Among the methods discussed in Section 3.4 one of the techniques are tested further on an additional case study. The assembly in the case study is adjusted in accordance with the results of the RCA. The assembly, the analyses and the results of the adjustment are described in Section 3.5.

Finally, in Section 3.6 the different methods and techniques for quality control and root cause analysis are discussed and compared.

3.2 Data and models

The methods outlined in the following sections will be applied on two case studies. The assemblies and the corresponding measurement data are presented in this section.

3.2.1 Case study 1

The first case is an assembly consisting of two parts called outer side panel and doorframe. The parts can be seen in the top of Figure 3.1. This assembly is only analysed in $x-$ and z-direction, since the assembly is not rigid in the y-direction, which is a necessary condition for some of the diagnosis methods considered in Section 3.4. A fixture is used to position both parts. In Figure 3.1 the locators in xz-direction are marked with black triangles. Both parts are fixed in z-direction using a pin/hole contact (labelled B1/C) and a pin/slot contact (labelled B2). The pin/hole contacts are also used for positioning the parts in x-direction. A pin/slot is a pin placed in a slot, i.e. an oval hole. Therefore the part is only restricted in one direction using this kind of locator. A pin/hole locator restricts the part in two directions.

After the positioning, the parts are welded together. When the assembly is measured, it is fixed in zx-direction using the pin/hole contact on the doorframe (B1) and the slot/pin contact on the side panel (B2), as shown in the middle part of Figure 3.1.

Four inspection points are used, marked by arrows in Figure 3.1, and three of these points are measured in z-direction as well as the x-direction. The fourth inspection point is only measured in x-direction.

The inspection data consist of 217 groups, where each group contains measurements from three consecutive cars. The data contain trends, see Figure 3.2. These trends may partially be caused by fixture faults, but if there are fixture faults causing variation, these faults will cause within group variation as well. Therefore, it is possible to estimate the variation caused by the fixtures by concentrating on the short-term variation only. The trends are therefore eliminated and the estimate of the covariance matrix is based on the within group variation.

The measurements are denoted $\boldsymbol{x}_{ij}$, $i = 1, 2, ..., m$ and $j = 1, 2, ..., n$, where $\boldsymbol{x}_{ij}$ is a vector consisting of inspection data for p inspection points on the jth item in the ith group. Here, $m = 217$ and $n = 3$. The n observations in each group are put together in the group mean,

$$\bar{\boldsymbol{x}}_i = \frac{1}{n} \sum_{j=1}^{n} \boldsymbol{x}_{ij}.$$

The inspection data can be decomposed into an overall mean, $\boldsymbol{\mu}$, a group effect, $\boldsymbol{\tau}_i$, and a error component, ϵ_{ij}, i.e.

$$\boldsymbol{x}_{ij} = \boldsymbol{\mu} + \boldsymbol{\tau}_i + \epsilon_{ij},$$

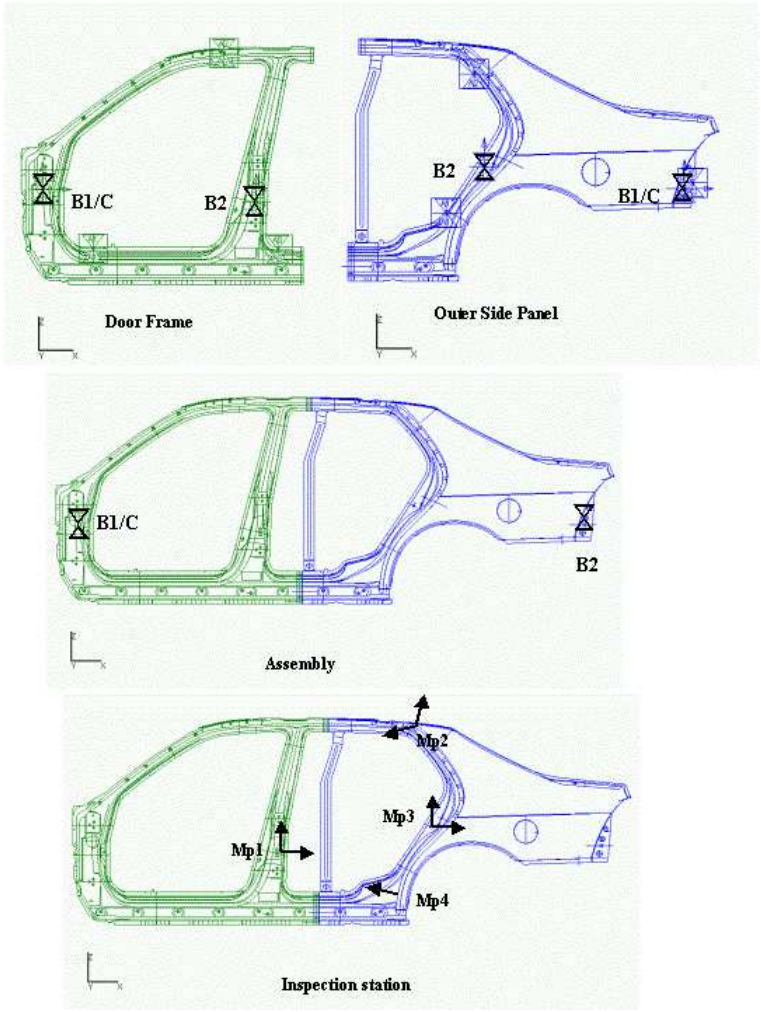

Figure 3.1: *Top: The side panel assembly consists of the door panel and the outer side panel. Middle: The assembly is positioned in xz-direction using the locators labelled B1 and B2. Bottom: The assembly is measured in four inspection points.*

and the covariance matrix of the data can consequently be expressed as the sum of the between group variation, Σ_τ, and the within group variation, Σ_ϵ, i.e.

$$\Sigma = \Sigma_\tau + \Sigma_\epsilon.$$

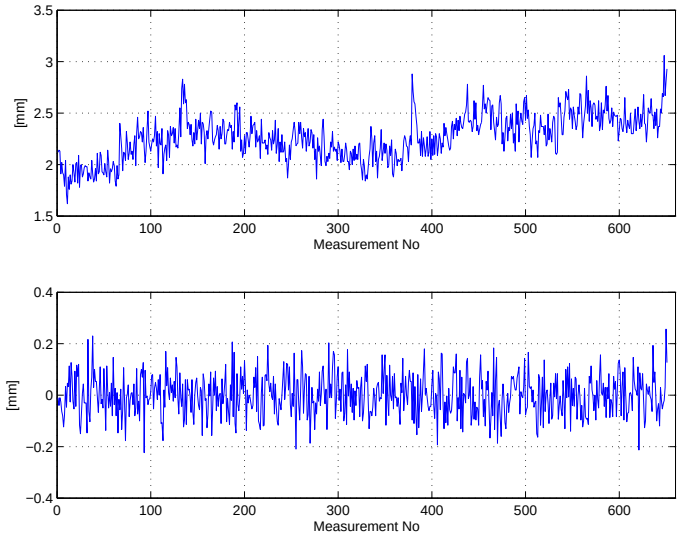

Figure 3.2: *Top: The original data from inspection point 2 in x-direction, side panel assembly. Bottom: The same data but with the trends eliminated.*

As mentioned before, the variation caused by the fixtures can be estimated by the within group variation, Σ_ϵ. To eliminate the trends, the group mean is subtracted from each observation in every group,

$$\boldsymbol{z}_r = \boldsymbol{x}_{ij} - \bar{\boldsymbol{x}}_i, \text{where } r = 1, 2, ..., mn,$$

This procedure gives $m * n$ measurements without trends and the p-variate vector $\bar{\mathbf{z}} = \mathbf{0}$, so the within group variation can be estimated as

$$\hat{\Sigma}_\epsilon = \frac{1}{m(n-1)} \sum_{r=1}^{mn} (\boldsymbol{z}_r)(\boldsymbol{z}_r)^T. \tag{3.1}$$

3.2.2 Case study 2

The second case study deals with an assembly where a rear bumper is joined with a vehicle floor, see Figure 3.3. The bumper is in yz-direction positioned by a fixture, using the locators labelled B1, B2 and C, and in x-direction by the contact (the contact points are labelled A1, A2 and A3) with the floor.

To monitor the assembly process 14 inspection points on the bumper are measured after the two parts are joined. During inspection the locators

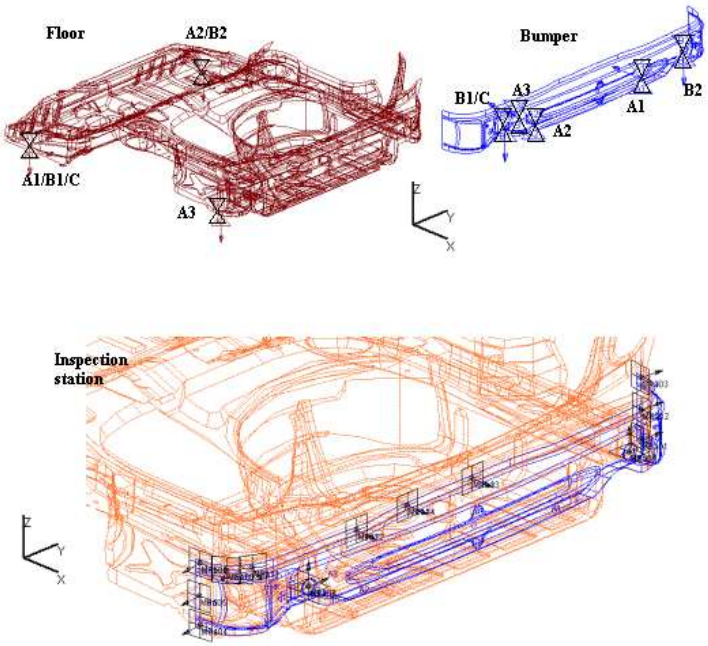

Figure 3.3: *The bumper and floor are assembled. Finally 14 points on the bumper are measured.*

of the floor are used to position the assembly. Hence, inspection points on the floor, if any, will not show any assembly variation even if the floor was incorrectly positioned during assembly. This variation will on the other hand be observed in the inspection point on the bumper. Therefore, the assembly process can only be monitored using inspection points on the bumper. The inspection data are, unlike case study 1, not arranged into subgroups. The data consist of 36 measurements of each inspection point, see Figure 3.4. It can be seen from the figure that there are considerable changes in the process after 16 measurements. There is much more variation in measurement 17 to 36, than in measurement one to 16. It is known that this variation is due to a variation in the contact between the bumper and the locator controlling translations in y-direction. That knowledge make the case study very suitable for testing different methods for RCA, since the results can be compared to this information. The case study is also well suited for testing and evaluation of MSPC-methods.

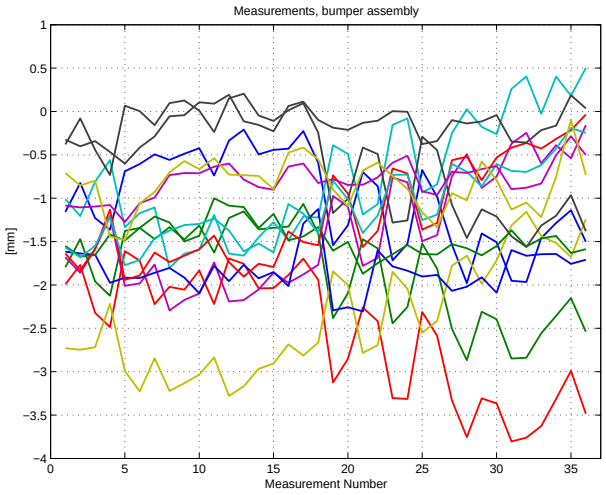

Figure 3.4: *Inspection data for 36 assemblies in 14 inspection points.*

3.3 Multivariate Statistical Process Control

In order to improve and maintain the quality of a product it is important to detect any changes in the process as soon as possible. There can be various causes of extra variation in a process. One of these possible reasons is fixture failure and in this section, an overview of methods to detect this type of variation is given. In Section 3.3.1-3.3.4 general methods to detect variation and offsets in the process are given, in Section 3.3.5 and Section 3.3.6 special methods designed to detect variation caused by fixture faults are considered.

The methods for statistical process control can be divided into univariate and multivariate procedures. The univariate methods are aimed at controlling measurements of one quality variable or inspection point. To control several related points at the same time it is convenient to use a multivariate control chart, and it is this kind of charts that is considered in this chapter.

A control chart consists of a statistic, which is plotted in the diagram for each observation, and corresponding control limits. If the statistic plots outside the control limits, the process is assumed to be out of control, and this implies that the process has changed. The probability of false alarm, α, i.e. the probability that the statistic plots outside the limits despite

the process remains in control, is depending on the significance level of the control limits. A usual choice is $\alpha = 1\%$ or $\alpha = 0.1\%$.

Since a multivariate control chart is used to control all the inspection points at the same time, it is sometimes complicated to identify the point or points that cause an alarm. In the regression adjustment method and the self-organizing map method, considered later in this chapter, this problem is partly solved. There are also many other methods that deal with this question, see for example Runger et al. (26), Jackson (19) and Hayter and Tsui (14).

3.3.1 T^2-chart

One of the most frequently used multivariate control charts is the T^2-chart. It is used to control the mean value of p inspection points. It is also sensitive to increased process variation.

The statistic

$$\chi_0^2 = n(\bar{\boldsymbol{x}} - \boldsymbol{\mu}_0)^T \boldsymbol{\Sigma}_0^{-1} (\bar{\boldsymbol{x}} - \boldsymbol{\mu}_0),$$

where $\boldsymbol{\mu}_0$ is a $p \times 1$ vector of in-control means and $\boldsymbol{\Sigma}_0$ is a $p \times p$ in-control covariance matrix, follows a χ^2-distribution with p degrees of freedom, see e.g. Montgomery (25). When the true population parameters are not known, the following statistic is used to form a Hotelling's T^2 control chart:

$$T^2 = n(\bar{\boldsymbol{x}}_i - \bar{\bar{\boldsymbol{x}}})^T \boldsymbol{S}^{-1} (\bar{\boldsymbol{x}}_i - \bar{\bar{\boldsymbol{x}}}).$$

This statistic was developed by Hotelling (16). Alt (2) showed that T^2 (times a constant) follows an exact F-distribution, and the upper control limit (UCL) is therefore given by

$$UCL = \frac{p(m+1)(n-1)}{n(mn-m-p+1)} F_{\alpha,p,mn-m-p+1},$$

where n is the number of observation in each sample, m is the number of samples taken and $F_{\alpha,p,mn-m-p+1}$ is the inverse of the F distribution function with p and $mn-m-p+1$ degrees of freedom, at the value of α. If the sample mean $\bar{\bar{\boldsymbol{X}}}$ and the sample covariance matrix $\boldsymbol{S}$ are estimated from a relatively large number of samples (at least 20 or 25) it is customary to use $\chi^2_{\alpha,p}$ as an upper control limit on the Hotelling T^2 chart.

Test on data

When using the data from the side panel assembly, with $p = 7$ inspection points, we concentrate on controlling the within group variation, so $\hat{\Sigma}_\epsilon$ from

Equation (3.1) on page 49 is used instead of S. In Figure 3.5

$$T_i^2 = (\boldsymbol{z}_i)^T \hat{\Sigma}_\epsilon^{-1} (\boldsymbol{z}_i)$$

is plotted for $i = 1, ..., 651$. Here, $\chi^2_{0.001,7}$ is used as an upper control limit. There are several observations above the control limit, so the process is said to be out of control. Since α, the probability of type I error is chosen to be 0.001 the expected number of false alarms is $0.001 * 651 = 0.651$ when the process is in control.

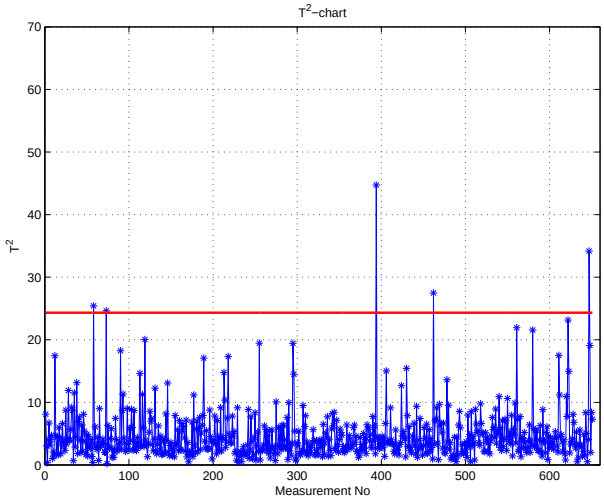

Figure 3.5: *Multivariate T^2-control chart based on within group variation for side panel assembly.*

The method is also applied on the bumper assembly data. Since the process is in an unacceptable stage during measurements 17 to 36, these data are not included in the estimates of the parameters. The multivariate T^2-chart, see Figure 3.6, shows a considerable change in measurement 17. However, the covariance matrix for the 14 inspection points is nearly singular. This fact makes the T^2-values after the 16th measurement very big. Often, a principal component analysis is recommended for this kind of data. That method is considered in the next section.

This example shows that the T^2-chart is an effective tool when it comes to detect changes in a process, especially when the changes affects several inspection points.

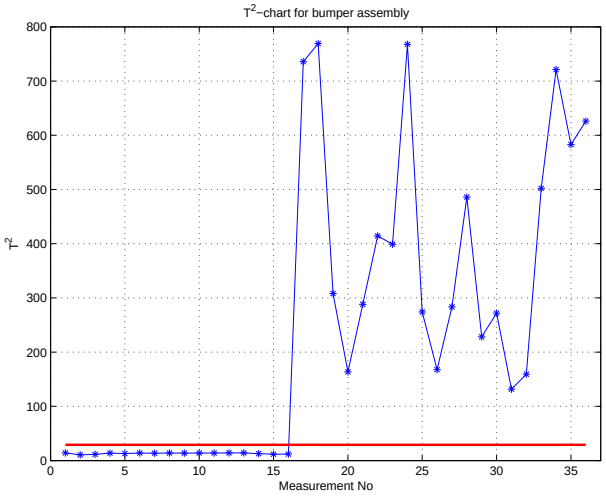

Figure 3.6: *Multivariate T^2-control chart, bumper assembly*

3.3.2 Principal Components and SPE

Principal Component Analysis (PCA) can be used to control a process as well as for diagnosing sources of variation, which is considered in Section 3.4.2.

The idea of PCA is to form a set of new variables, which are linear combinations of the old ones. The new variables, the principal components, are independent of each other. These principal components display different amounts of variance and usually, the variance of some of the components will be so small that they can be considered negligible. Therefore, the variation in the original variables can be described by a smaller number of new variables. The general objectives of PCA are reduction and interpretation of data.

In short, the PCA is performed by computing eigenvalues and eigenvectors of the covariance matrix, $\boldsymbol{\Sigma}$, of the original variables. An eigenvalue, λ_i, is a root of the characteristic equation

$$|\boldsymbol{\Sigma} - \lambda_i \boldsymbol{I}| = 0$$

and a the corresponding eigenvector is a non-zero vector $\mathbf{v}_i$, satisfying

$$\boldsymbol{\Sigma} \boldsymbol{v}_i = \lambda_i \boldsymbol{v}_i.$$

The eigenvalues and their corresponding eigenvectors are sorted in order of size. The principal components, $\boldsymbol{Y}$, are formed in the following way

$$Y_i = \boldsymbol{v}_i^T \boldsymbol{X},\ i = 1, 2, ..., p$$

where $\boldsymbol{\Sigma}$, the covariance matrix of $\boldsymbol{X}$, has eigenvalues

$$\lambda_1 \geq \lambda_2 \geq ... \geq \lambda_p,$$

with corresponding eigenvectors $\boldsymbol{v}_i$) with unit length. Often, a few of the principal components contain the main part of the total variance in the population. The ith principal component, $\boldsymbol{Y}_i$, contains

$$100 * \frac{\lambda_i}{\lambda_1 + \lambda_2 + ... + \lambda_p}$$

percent of the total variation. If the major part of the variance is contained in the first k principal components, then these components may replace the p original variables, without loosing too much of the information. To determine k, it is possible to perform a χ^2-test, see Jackson (18).

A more elaborate discussion of principal component analysis will be found in Johnson and Wichern (21).

To control the process using PCA the statistic

$$T^2_{pca}(i) = (\bar{\boldsymbol{X}}_i - \bar{\bar{\boldsymbol{X}}})^T P P^T \Sigma^{-1} P P^T (\bar{\boldsymbol{X}}_i - \bar{\bar{\boldsymbol{X}}})$$

is used, see Jackson (20). Here, $P = [\boldsymbol{v}_1 | \boldsymbol{v}_2 | ... | \boldsymbol{v}_k]$ is the matrix of the first k eigenvectors. The statistic is χ^2-distributed and the upper control limit is given by $\chi^2_k(\alpha)$. The k principal components used span a subspace containing the variation described of these principal components, and the T^2_{pca}-statistic is used to control the quantity of this variation. If the nature of the variation changes, for example there is increased variation outside the subspace spanned by the principal components, the control diagram does not detect that. This means that there is need for a chart controlling the size of the residual, i.e. the distance between an observation and the subspace, see Figure 3.7 for an illustration of the residual. Since $PP^T\boldsymbol{x}$ is a projection of an observation $\boldsymbol{x}$ on the subspace, the following statistic can be used:

$$SPE_{pca} = (\boldsymbol{x} - PP^T\boldsymbol{x})^T(\boldsymbol{x} - PP^T\boldsymbol{x})$$

According to Jackson (20), the SPE statistic is Q-distributed and the control limit is given by

$$Q_\alpha = \phi_1 (c_\alpha \frac{\sqrt{2\phi_2 h_0^2}}{\phi_1} + \frac{\phi_2 h_0 (h_0 - 1)}{\phi_1^2} + 1)^{\frac{1}{h_0}},$$

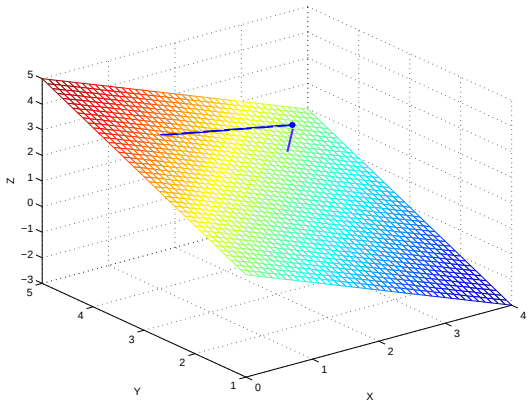

Figure 3.7: *An observation (*) plot outside the principal component subspace. The SPE_{pca}-statistic measure the distance between the observation and the principal component subspace.*

where c_α is the inverse of the standard normal cumulative distribution function,

$$\phi_1 = \sum_{i=k+1}^{p} \lambda_i, \qquad \phi_2 = \sum_{i=k+1}^{p} \lambda_i^2, \qquad \phi_3 = \sum_{i=k+1}^{p} \lambda_i^3$$

and

$$h_0 = 1 - \frac{2\phi_1\phi_3}{3\phi_2^2}.$$

Test on data

In Figure 3.8, the T^2_{pca} and SPE_{pca}-statistics for the side panel assembly are plotted. No between group variations are included, i.e. the PCA is based on Σ_ϵ. The matrix P consists of the three first principal component vectors, $P = [\boldsymbol{v}_1|\boldsymbol{v}_2|\boldsymbol{v}_3]$, and these three together contain 86% of the total variation. The UCL is given by $\chi^2_3(0.001)$.

This chart gave some fewer alarms compared to the usual T^2-chart, used in Section 3.3.1. The reason for this is that only 86% of the total variation is included in the principal components. Despite this, there are indications that the process is out of control. The usual T^2-chart alarmed five times, while the T^2_{pca}-chart alarmed three times.

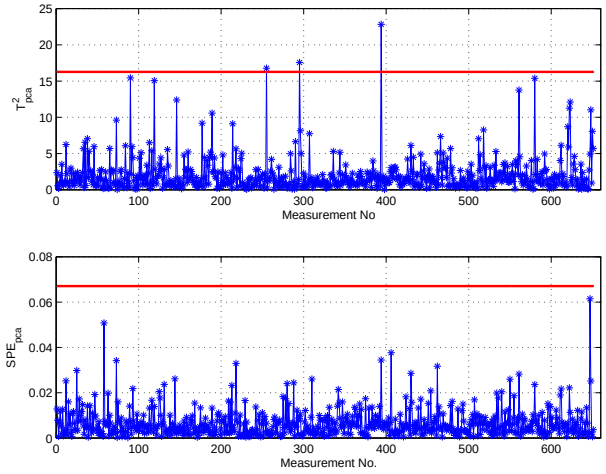

Figure 3.8: *On top a T^2_{pca}-chart and below a SPE_{PCA}-chart for the side panel assembly.*

The method is also tested on the bumper assembly, and the result can be seen in Figure 3.9. The mean value and the covariance matrix are estimated from the first 16 measurements. The chart gives an alarm in measurement 19. The SPE-chart gives an alarm as well, which indicates that the variation no longer is contained in the subspace spanned by measurement one to 16. In this case, the fixture related fault caused an increased variation after the 16:th measurement. But the fault also implied a different kind of variation compared to the one spanned by the first 16 measured objects, and that causes an alarm in the SPE_{PCA}-chart. When comparing this chart to the usual T^2 chart a major difference is that the increase after observation 16 is much more moderate when PCA is used. That is because the problem with the almost singular covariance matrix is avoided using PCA.

3.3.3 Regression adjustment

Regressing one variable on all the others and then control the regression residuals is an approach for MSPC, considered by Hawkins (12). In regression adjustment separate charts for controlling mean value and variation can be used, which may be advantageous. The method is especially well suited when only a shift in some of the variables is expected. This is usually not the case if the error is fixture related, since a movement in one locator often affects many inspection points, but the method is nevertheless tested on the case studies. An overview of the method is also given by Mont-

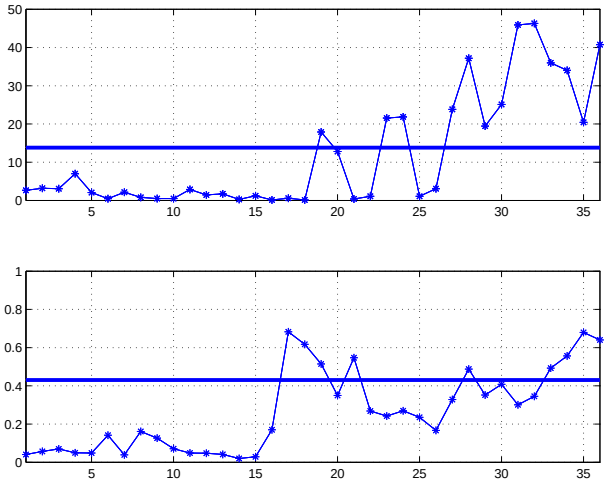

Figure 3.9: *On top a T^2_{PCA}-chart and below a SPE_{PCA}-chart for the bumper assembly.*

gomery (25).

The residuals, $\mathbf{r}_i = \hat{\mathbf{X}}_i - \mathbf{X}_i$, $i = 1, ..., p$, are calculated for each inspection point i using a usual multiple linear regression for each inspection point, i, $i = 1, ..., p$, i.e.

$$\hat{\mathbf{X}}_i = \boldsymbol{\alpha} + \sum_{i \neq j} \boldsymbol{\beta}_j \mathbf{X}_j.$$

The standardized residual of the regression of one variable on the other variables will follow a $N(0, 1)$-distribution when the process is in control. Therefore, the control charts are similar to univariate control chart. But since the regression residuals are plotted the correlation between different variables is taken into account.

Test on data

The regression analysis for the side panel assembly is based on the measurements with removed trends, i.e. $\boldsymbol{z}_i$, $i = 1, ...651$, is considered. The residuals are controlled by an EWMA-chart, see Figure 3.10, and a moving range chart, see Figure 3.11. The EWMA-charts give only a few alarms, while the moving range-charts signals more often. This indicates that the

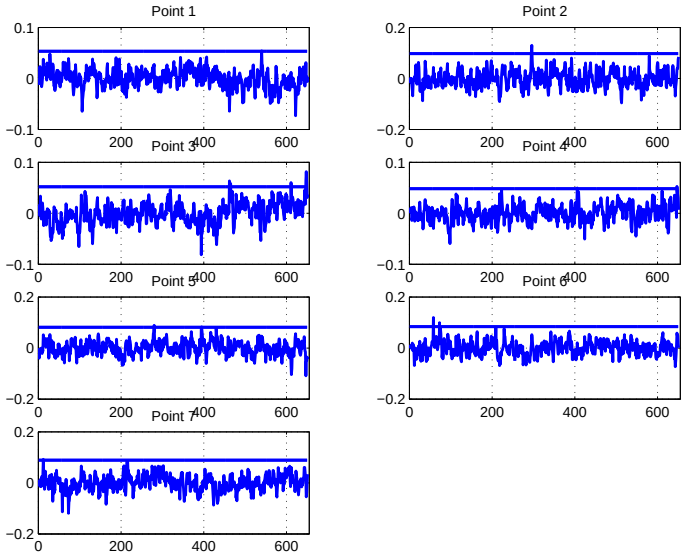

Figure 3.10: *Regression adjustment case study 1, EWMA chart for controlling the regression residuals.*

major problem in the side panel assembly is too much variation, not shifts in the mean value.

The regression adjustment is also applied to nine of the inspection points on the bumper assembly. In this case it is known that the major problem is caused by increased variation after measurement 16. The residuals are therefore controlled with a moving range chart, see Figure 3.12. The numbers of alarms are not increasing distinctly after the 16:th measurement. A reason of that may be that the root cause affects several variables, not only one or two. These kinds of charts perform best when only one variable is likely to be affected by the variation.

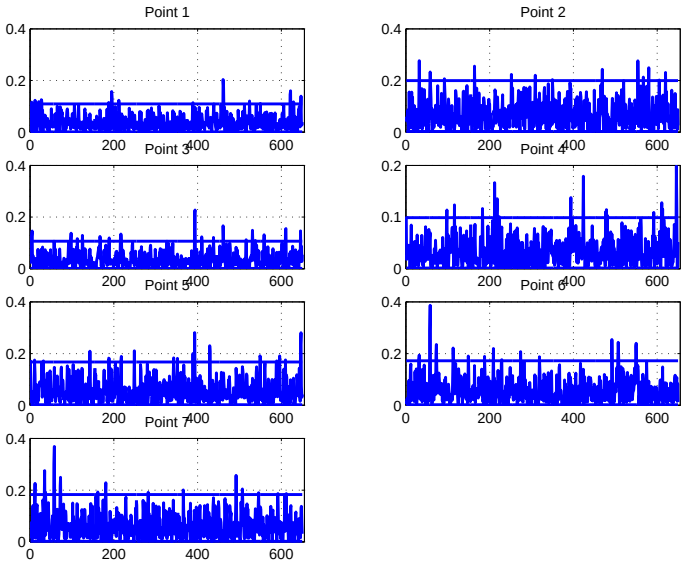

Figure 3.11: *Regression adjustment case study 1, moving range chart for controlling the regression residuals.*

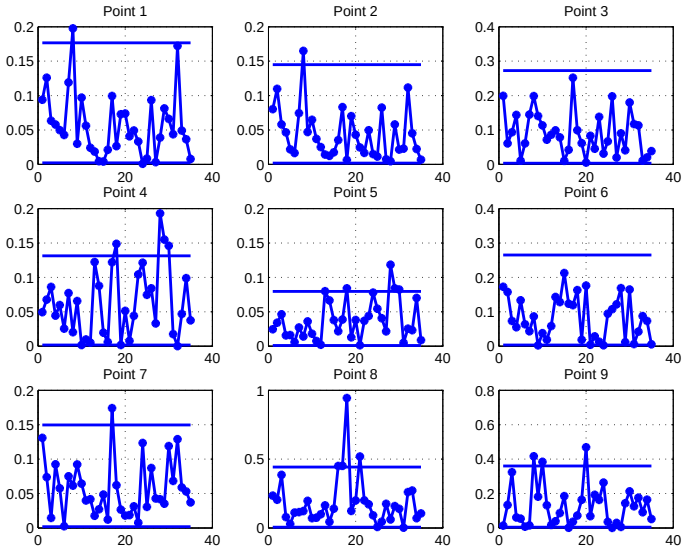

Figure 3.12: *A moving range chart of the regression residuals, bumper assembly.*

3.3.4 Self Organizing Maps

A Self Organizing Map (SOM) is a special type of artificial neural network (ANN) that can be used for multivariate process control and in some cases also for fault identification. A neural network is an adaptive model for non-linear multivariate data. It can learn from the data and generalize the things learned. An ANN consists of a number of neurons in different layers. Each neuron has an individual weight vector and all neurons have connections to other nodes. There are two different kinds of ANN; the supervised ANN and the unsupervised ANN. In supervised learning the system directly compares the network output with a known correct or desired answer, whereas in unsupervised learning the desirable output is not known. ANN is studied by for example Haykin (13).

The SOM was developed by Kohonen (23), and is one of the most popular network models. It is based on unsupervised, competitive learning. It provides a topology preserving mapping from high dimensional input vectors to a low dimensional (usually two dimensional) grid of neurons. Each neuron is represented by a weight vector of the same size as the input vector.

The SOM is trained iteratively, Ahola et al. (1). In each step the Best Matching Unit (BMU) for the input vector is found by comparing the input vector, $\boldsymbol{x}$, with the weight vector, $\boldsymbol{m}$, of every neuron in the net. The neuron closest to the input vector wins, i.e. if the BMU is labelled $\boldsymbol{m}_c$,

$$||\boldsymbol{x} - \boldsymbol{m}_c|| = \min_i \{||\boldsymbol{x} - \boldsymbol{m}_i||\}.$$

Usually, the Euclidian norm is used. The weights of the BMU as well as the weights of the neighbours of the BMU are updated to be more similar to the input vector,

$$\boldsymbol{m}_i = \boldsymbol{m}_i + \alpha(t) h_{ci}(t)(\boldsymbol{x} - \boldsymbol{m}_i),$$

where $\alpha(t)$ is the learning rate and h_{ci} is a neighbourhood function around the winner unit c. Both the learning rate and the neighbourhood function are decreasing function of time. By this procedure the net is formed to estimate the distribution of the input data.

Ultsch and Siemon (34) use a unified distance matrix (u-matrix) to visualize the structure of a SOM. The mean difference between a neuron and its neighbours is calculated. The result of these calculations is presented using a two-dimensional grey-scale picture. A dark area can for example mean that there are small differences between the neurons in the region, while a bright area means that the neurons in that region are not very similar

to each other. By this procedure the dark areas can be identified as clusters.

If the SOM is trained on data from the normal operation state as well as on data from different erroneous states the clusters corresponding to these faulty states can be labelled with the fault type or even better, the root cause of the fault.

After the SOM is trained then the net can be used for process control. The inspection data vectors are fed in to the net and the BMU is identified. When the BMU is a node labelled "undesired state" the process is out of control. Plotting the trajectory of the BMU for each measurement vector can be a way of monitoring the process. Since the undesired states are labelled with root causes this procedure may help in fault detection.

If the SOM is trained using measurement vectors describing the normal state of the process only, then the net is forming a mapping of the "normal operation" input space. In order to detect a faulty situation the quantization error can be studied, Ahola et al. (1). The quantization error for unit i, $q_i = \sqrt{\sum_{k=1}^{p}(x_k - m_{ik})^2}$, is the distance between the input vector and the BMU. A large quantization error implies that the process no longer is in the "normal operation" space. This method gives no information of the root cause of the fault.

Test on data

When it comes to applying SOM to data in order to perform process control the results seem to be highly dependent on the number of nodes chosen, what subset of the data that are used for training and so on. Perhaps, SOM is best suited for use by an expert in the area, who can analyse those questions and find the appropriate settings.

Having this in mind, the method is tested only on the bumper assembly. The net is trained using measurement one to 16, i.e. data representing the normal state of the process are used. These data are also used to estimate the mean and standard deviation of the process in order to standardize data. The measurements used for calculating the quantification error are not included during the training phase. Usually a SOM is supposed to be trained on a much larger data set then the one used here, but still, it gives an idea of how the SOM works.

In Figure 3.13 is the quantization error plotted. The first four bars is the quantification error for data before measurement 16, while the remaining

ones are the quantification errors for data after the 16:th measurement. The quantification errors obviously increase after measurement 16, indicating that the process is no longer in the normal operation state.

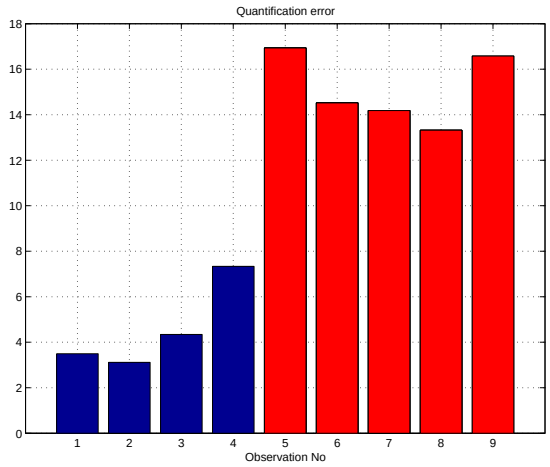

Figure 3.13: *Quantization error for a SOM for bumper assembly. The first four bars correspond to observations before the fixture failure occurred, while the remaining five bars correspond to observations after that fault.*

3.3.5 Fixture failure index

In this section, as well as in the following one, special methods for examining the occurrence of fixture faults are considered.

Carlson et al. (4), introduce a fixture failure index in order to determine if a fixture failure is present. To calculate this index the sensitivity matrix, A, must be known. The sensitivity matrix describes the connection between a displacement in the locators and the resulting displacement in the inspection points. This means that a displacement, $\mathbf{d}$, in the inspection points can be expressed as

$$\mathbf{d} = A\delta,$$

where δ is a small displacement in the locators. The matrix A is calculated analytical or numerical, see Carlson and Söderberg (5).

In order to calculate the fixture failure index the observations are split into two orthogonal subspaces, the failure subspace and the noise subspace.

The failure subspace contains the fixture errors and the residual errors, and the noise subspace contains no fixture errors. A measurement $\mathbf{x}$ can accordingly be written as

$$\mathbf{x} = U_r U_r^T \mathbf{x} + U_{p-r} U_{p-r}^T \mathbf{x},$$

where U_r is an orthonormal basis for the r-dimensional column space of the sensitivity matrix A and U_{p-r} is an orthonormal basis for the $(p-r)$-dimensional null space of A^T.

This decomposition makes it possible to calculate the fixture failure variation index, Ψ, by comparing the amount of variation in the failure subspace with the total variation;

$$\Psi = \frac{\text{Trace}(U_r U_r^T \Sigma_x U_r U_r^T)}{\text{Trace}(\Sigma_x)}.$$

A value of Ψ close to one indicates a fixture fault. When there is no fixture fault variation, the expected value of Ψ is r/p.

Since an estimate of the covariance matrix must be used, an uncertainty in the calculations arise. This uncertainty is taken care of by introducing an approximate confidence interval, derived by Carlson et al (4). The confidence interval for the fixture failure variation index is, when $\alpha = 0.05$, given by

$$\hat{\Psi} \pm 1.96\sqrt{\tau^2} \quad \text{where}$$

$$\hat{\tau}^2 = 2\frac{(1-\hat{\Psi})^2 \text{Trace}(U_r^T S_x U_r)^2 + \hat{\Psi}^2 \text{Trace}(U_{p-r}^T S_x U_{p-r})^2}{(n-1)(\text{Trace}(S_x))^2}.$$

Test on data

In Figure 3.14 the variation index, Ψ, is plotted for the side panel assembly. The index is calculated for each group of observations using a moving estimate of the within variance-covariance matrix over seven groups.

If there is no fixture fault the expected value of the index is r/p, where r is the rank of the sensitivity matrix A and p is the number of inspection points. This value corresponds to the horizontal limit in Figure 3.14. In Figure 3.14 the fixture failure index and the 95% confidence interval are plotted. The index is based on the within group variation, i.e. $S_x = \hat{\Sigma}_\epsilon$. The index indicates that a fixture failure may be present.

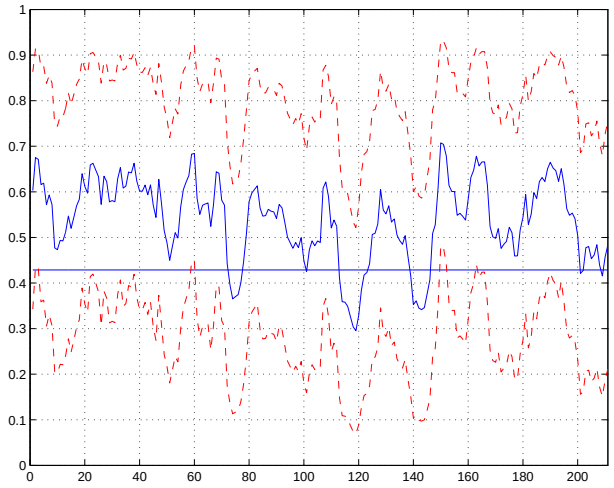

Figure 3.14: *Fixture failure variation index, side panel assembly.*

This method is also applied on the bumper assembly. Since the data is ungrouped the covariance matrix is calculated by a moving estimate. The index is above the limit for all groups, see Figure 3.15. The index is even closer to one after the 16:th measurement. The increased variation after measurement 16 is consequently probably due to fixture faults. This conclusion is in accordance with the information known; there is a noticeable fixture fault in measurement 16 to 36.

3.3.6 Fixture failure subspace chart

To control the variation that originates from the fixtures, the amount of variation in the fixture failure subspace can be studied. The fixture failure subspace is spanned by U_r, the orthonormal basis for the r-dimensional column space of the sensitivity matrix A. The vectors that span A can be collected into the matrix P, and the same method as in Section 3.3.2 can be used by considering the statistics

$$T^2_{fixture} = (\boldsymbol{x} - \bar{\boldsymbol{x}})^T P P^T \Sigma^{-1} P P^T (\boldsymbol{x} - \bar{\boldsymbol{x}}),$$

and

$$SPE_{fixture} = (\boldsymbol{x} - P P^T \boldsymbol{x})^T (\boldsymbol{x} - P P^T \boldsymbol{x}).$$

The control limit for the $T^2_{fixture}$-chart is $\chi^2_r(\alpha)$. For the SPE-chart a control limit is not yet developed.

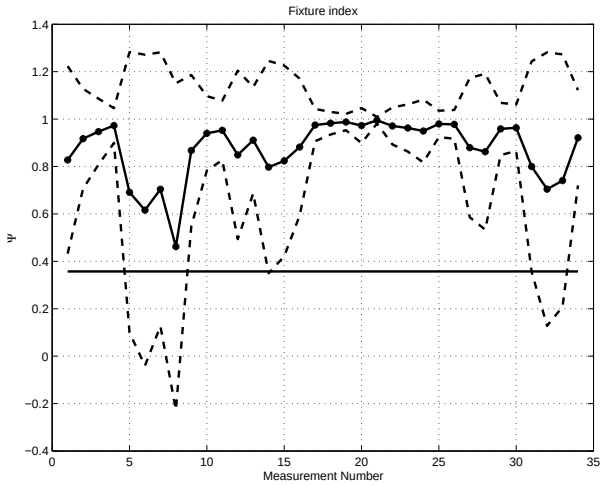

Figure 3.15: *Fixture failure variation index, bumper assembly.*

Test on data

In Figure 3.16 the $T^2_{fixture}$-statistic for the outer panel assembly is plotted. As a control limit $\chi^2_r(0.001)$ is used. The $SPE_{fixture}$-statistic measure the amount of variation that are not contained in the fixture failure subspace.

The chart in Figure 3.16 is based on measurements with the trends eliminated, i.e. $\boldsymbol{z}_i$, $i = 1, ..., 651$. The chart indicates that there is too much variation in the fixture failure subspace.

In Figure 3.17 the $T^2_{fixture}$ is plotted for the bumper assembly. The chart alarms before measurement 16 (i.e. before the known fixture related error) and indicates, just like the fixture index, that there are some fixture related errors in measurement one to 16 as well. After measurement 16 there is a considerable change in $T^2_{fixture}$ and it is obvious that there is increased variation in the fixture failure subspace.

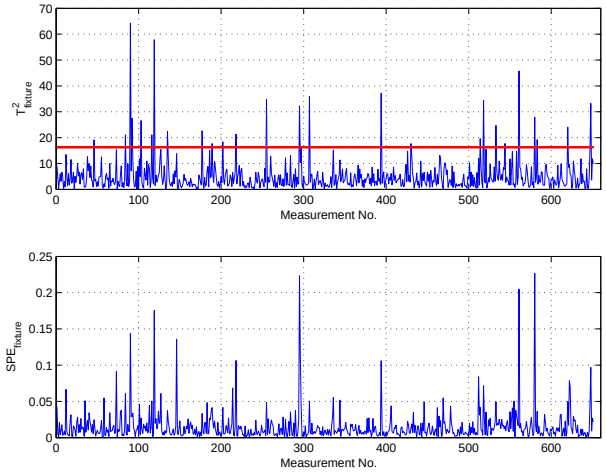

Figure 3.16: $T^2_{fixture}$- *and* $SPE_{fixture}$*-chart to control the variation in the fixture failure subspace, side panel assembly.*

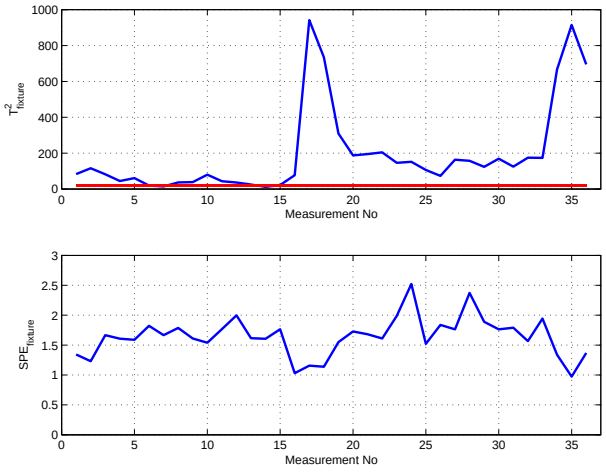

Figure 3.17: $T^2_{fixture}$- *and* $SPE_{fixture}$*-chart to control the variation in the fixture failure subspace, bumper assembly.*

3.4 Fixture diagnosis

The methods described in Section 3.3 are used to control the process. Usually, the root cause of a problem detected by statistical process control methods is not known. The fault can depend on material, external circumstances, fixture faults and so on. In the previous section some methods for discovering fixture related faults were given. If a process is out of control and the fixture fault index is below the corresponding limit the fixtures can be excluded from the list off possible root causes. If the index is above the limit the root cause is probably fixture related and then it is of course desirable to find out what fixture and what locator that caused the problem. In this section some suggestions of how to identify the cause of fixture related faults are given.

The methods of fixture diagnosis can be divided into two separate groups of approaches; the methods that require knowledge of the assembly process, coordinates of inspection points et cetera and the data based methods that only utilize inspection data for diagnosis.

3.4.1 Root Cause Analysis

One way to find the reason of the unwanted variation in the inspection points would be to estimate the variation in each locator of the fixtures involved. The locator or locators affected by most variation is said to be the root cause of the variation. This approach is considered by Carlson and Söderberg (6), and requires knowledge of the assembly process.

The inspection data are supposed to have covariance matrix Σ_x. When the fixture failure index is large, we will assume that Σ_x can be written as

$$\Sigma_x = A\Lambda_\delta A^T + \sigma^2 I_p, \tag{3.2}$$

where A is the sensitivity matrix and Λ_δ is a diagonal locator covariance matrix. The model

$$\Sigma_x = A\Sigma_\delta A^T + \sigma^2 I_p,$$

can also be used. Here, the locator covariance matrix Σ_δ is a full matrix. However, the condition that the locators will be independent, and consequently that the covariance matrix will be diagonal, is usually no limitation, since variation in one locators seldom affects other locators. Therefore, the model described in Equation (3.2) will be used.

The measurements are supposed to follow a multivariate normal distribution. If it is possible to estimate the elements in Λ_δ, the diagnosis can be

accomplished. A maximum likelihood estimate of Λ_δ and σ^2 can be found by maximizing the likelihood function

$$l(\boldsymbol{x};\boldsymbol{\mu},\Sigma_x) = -\frac{n}{2}\log\det(2\pi\Sigma_x) - \frac{n}{2}\text{Trace}(\Sigma_x^{-1}S_x) - \frac{n}{2}\text{Trace}(\Sigma_x^{-1}(\bar{\boldsymbol{x}}-\boldsymbol{\mu})(\bar{\boldsymbol{x}}-\boldsymbol{\mu})^T).$$

The maximization may be done numerically by Fishers scoring method; more about this method can be read in Jöreskog (22). Large sample confidence regions for the estimates may be constructed.

Unfortunately, it is not always possible to separate variation from different locators. The reason for this is that two locators can cause the same dimensional deviation in the inspection points. If this is the case, the assembly is said to be incomplete diagnosable. The conditions for complete diagnosability implies the following relation

$$A\Lambda_1 A^T + \sigma_1^2 I_p = A\Lambda_2 A^T + \sigma_2^2 I_p \Leftrightarrow \Lambda_1 = \Lambda_2 \text{ and } \sigma_1 = \sigma_2.$$

This condition can be rewritten as $T = A \otimes A$ have full rank, Carlson and Söderberg (6). Further, the number of inspection points must exceed the number of locators analysed. If a full locator covariance matrix is used, the condition on A for complete diagnosability is strengthened to A having full rank. If the assembly is not completely diagnosable, it is still possible to perform a diagnosis. By solving the linear programming problems

$$\max_\lambda \boldsymbol{\lambda}_k$$
$$L\boldsymbol{\lambda} = L\boldsymbol{\lambda}^*,\ \boldsymbol{\lambda} \geq 0$$

and

$$\min_\lambda \boldsymbol{\lambda}_k$$
$$L\boldsymbol{\lambda} = L\boldsymbol{\lambda}^*,\ \boldsymbol{\lambda} \geq 0$$

for each k, the minimal and maximal possible locator variance can be found. Here, L is an orthonormal basis matrix, V_r, for the r-dimensional column space of T^T and λ^* is a particular solution of the problem.

The estimation of locator variances is also considered by Ding et al. (11). They rewrite Equation (3.2) as

$$vec(\Sigma_x) = T\,vec(\Lambda_\delta) + vec(I)\sigma^2.$$

Using the notation $\mathbf{B} = [T\,vec(I_p)]$ and $\mathbf{d} = vec(\Sigma_x)$ this can be written as

$$\mathbf{B}\lambda^* = \mathbf{d},$$

and the the equation is solved by multiplication with the inverse of $\mathbf{B}$.

Test on data

The outer side panel assembly considered in Section 3.2 is incompletely diagnosable, and the minimal and maximal variation for each locator can be seen in Figure 3.18. The method by Carlson and Söderberg (6) is used for this case. The variation is calculated from measurement 53 to measurement 60, which is a period with a high fixture failure index. The horizontal limit in the figure correspond to $6\sigma = 0.5$ mm, which seems to be reasonable to use as a an upper limit for the allowable variation in a locator. As seen in

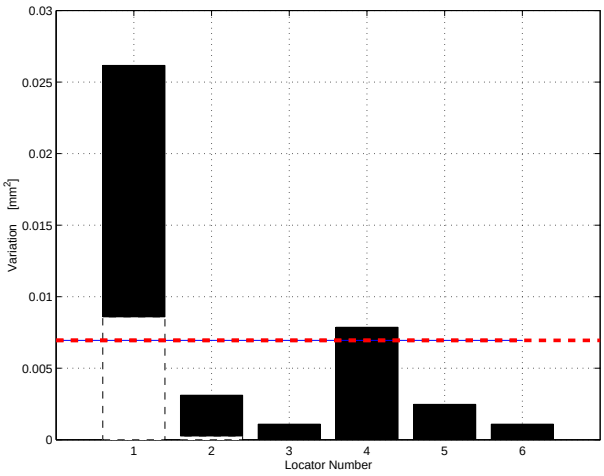

Figure 3.18: *Minimal and maximal variation in the locators due to incomplete diagnosability, side panel assembly. The extension of the dark area is from the minimum variance to the maximum variance.*

Figure 3.18, the interval from minimal to maximal variation for locator 1 is the only one which is above the limit. Therefore, this locator is pointed out as the main root cause. Locator 1 is a hole in the front part of the assembly, controlling the assembly in z-direction.

The methods are applied on the bumper assembly as well. The assembly is completely diagnosable. Here, both the estimates by Carlson and Söderberg (6) and by Ding et al. (11) are tested. The estimates can be seen in Figure 3.19. The first bar in each pair corresponds to the estimate developed by Carlson and Söderberg and the second one to the estimate by Ding et al.. Locator number six is the one containing most variation according to both estimates. There is also much variation in the first locator according to the second method. The sixth locator is a pin/hole contact

controlling translation in y-direction. In this case study there is a key; the

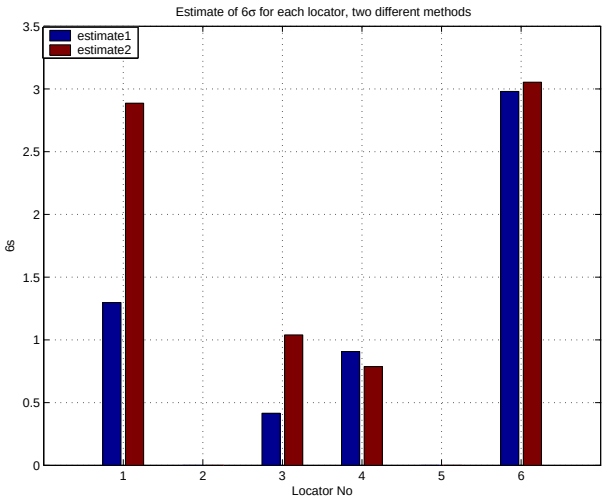

Figure 3.19: *Estimate of* 6σ *for the bumper assembly, measurement 17 to 36. The first bar in each pair corresponds to the estimate by Carlson and Söderberg, while the second one corresponds to the estimate by Ding et al.*

adjustment made was a correction of the pin/hole contact, i.e. the sixth locator in Figure 3.19. This adjustment reduced the variation in the measurements. This locator was pinpointed as the locator with most variation by both methods. However, the method by ding et al. indicated almost as much variation in the first locator.

There is also considerably variation in locator one, three and four. The fixture index indicated that there were fixture related variations in the process in measurement one to 16, i.e. before the variation in locator six occurred. Possibly the variation in these measurements could have been reduced by an adjustment of locator one.

3.4.2 Principal Component Analysis

In Section 3.3.2 PCA was described and utilized as a tool for process control. However, it is also possible to identify the sources of variation using PCA. Hu and Wu (17), propose that the result of a PCA can be interpreted by plotting the elements of each eigenvector at the respective inspection point location. If the normal directions of the inspection points are of opposite

signs, it is important to include this information in the analysis. It is convenient to plot the eigenvector times the sign of the normal direction of the respective inspection point. This approach is data based, so when using this method there is no need to calculate the sensitivity matrix used in Section 3.4.1.

The PCA is conducted on the estimated joint covariance matrix, S, for the inspection points evaluated in all directions. This seems to be a more attractive approach than the method conducted by Hu and Wu (17). Their

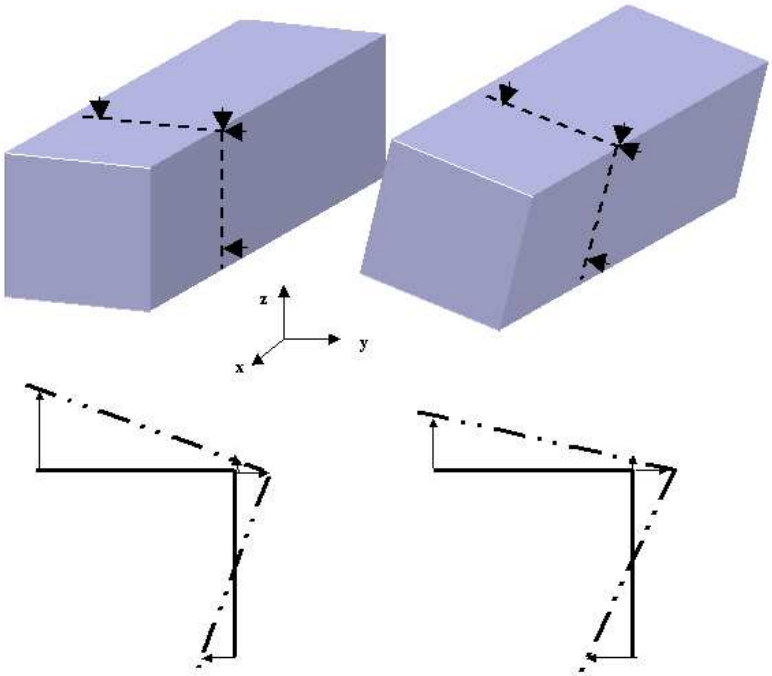

Figure 3.20: *Top: A box with four inspection points. To the right the box is rotated. Bottom: Principal components. To the left, based on the joint covariance matrix and to the right, based on separate covariance matrices. Observe that the right angle between the sides of the rotated box (illustrated by the dotted line) is preserved in the left picture, but not in the right one.*

method is based on separate PCAs on the covariance matrix for the inspection points in each direction. The difference is illustrated in the following

example. Consider a box with four inspection points, see the upper part of Figure 3.20. Two of the points are evaluated in the y-direction, and two are evaluated in z-direction. The box is rotated around the x-axis as shown in the right-hand upper part of Figure 3.20. In the bottom part of Figure 3.20 the principal components for this rotation are outlined. If the principal components are based on the joint covariance matrix for the four inspection points the geometry of the box is preserved. If the PCA is based on the two separate covariance matrices, the relation between the y-plain and the z-plain of the box is lost, and less information of the deviation can be extracted.

If the separate matrices are considered it is difficult to compare the amount of variation explained by the principal components in the different directions. Therefore, when comparing the length of the eigenvectors of the different covariance matrices, the geometric proportions between the movements in x- and z-directions are not preserved.

Test on data

The analysis is now applied to the case studies. As before, only the within group variation, Σ_ϵ, is considered in the side panel assembly, and the principal component analysis is conducted on this matrix. This results in two principal components that together contain 78% of the total variation. In Figure 3.21 and Figure 3.22 the elements of the eigenvectors are plotted at the respective inspection point location. The first eigenvector, representing 58% of the total variation, corresponds mainly to a translation in z-direction, see Figure 3.21. The second eigenvector corresponds mainly to a translation in x-direction, see Figure 3.22. These translations are though combined with rotations, since the arrows, representing movements in different inspection points, are of unequal length.

The first principal component, explaining much of the variation in the assembly, corresponds mainly to a translation in z-direction. The conclusion must be that the root cause is one of the locators that position the assembly in z-direction. In the previous section was locator number one pointed out as the root cause. This locator was positioning the side panel in z-direction. However, the interpretation of the analysis is not completely obvious, since the translation is combined with a rotation.

The method is also applied to the bumper assembly. Here is the interpretation of the result more clear. In Figure 3.23 is the first principal

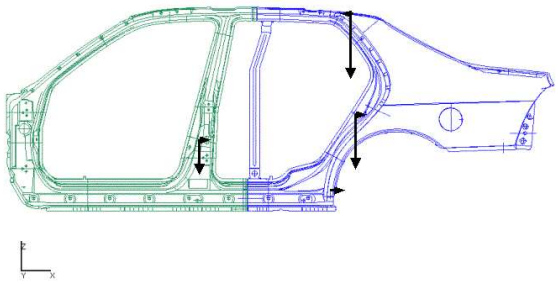

Figure 3.21: *The first eigenvector, representing 58% of the variation, side panel assembly.*

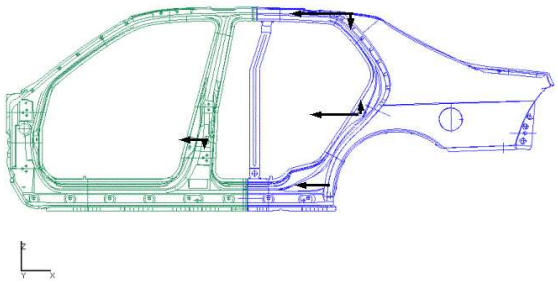

Figure 3.22: *The second eigenvector, representing 20% of the variation, side panel assembly.*

component drawn. This component explains 90% of the variation in data and indicates that there has been a translation in y-direction. This is in agreement with the conclusion drawn in Section 3.4.1.

This method is illustrative and no sensitivity matrix is needed. How-

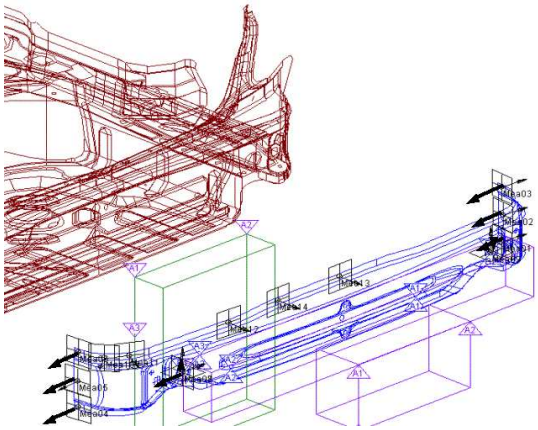

Figure 3.23: *The first principal component. Contains 90% of the variation, bumper assembly.*

ever, the method does not give a result as exact as the methods described in Section 3.4.1. This visual RCA is best suited for detecting single locator fault for small assemblies in one station (to avoid reorientation).

3.4.3 Designated Component Analysis

Designated Component Analysis (DCA) is an approach to fixture fault analysis developed by Camelio and Hu (3). DCA requires knowledge of the sensitivity matrix A. It is aiming to identify multivariate patterns, just like the PCA. This is achieved by defining a set of mutually orthogonal variation patterns with known physical interpretations. In sheet metal assembly processes, the physical interpretations are usually rigid body motion. Hence, the assembly variation can be decomposed in terms of all rigid body motions.

The designated patterns, denoted $\mathbf{d}_i$, $i = 1, ..., p$, span the subspace of the sensitivity matrix A. Their corresponding designated components, $\mathbf{w}_i$, can be calculated from inspection data $\mathbf{X}$ in the following way:

$$\mathbf{w}_i = \mathbf{d}_i^T * \mathbf{X},\ i = 1, ..., p$$

The inspection data can then be expressed as the sum of rank one matrices:

$$\mathbf{X} = \mathbf{P}_1 + \mathbf{P}_2 + ... + \mathbf{P}_p$$

where

$$\mathbf{P}_i = \mathbf{d}_i * \mathbf{w}_i,\ i = 1, ..., p.$$

Using this decomposition, the multivariate variation contained in $\mathbf{X}$ can be separated into p terms, each corresponding to a designated pattern.

When the designated components are calculated they can be analysed and removed from the original data. The remaining variation, contained in the residuals, $\mathbf{R} = \mathbf{X} - \sum_i \mathbf{P}_i$, can be analysed by applying the principal component analysis described in the previous section to the residual covariance matrix $\mathbf{S_R}$.

Test on data

When applying DCA to the side panel assembly described in Section 3.2 the three first designated patterns, corresponding to rigid body motions, are obtained. These span the subspace of the sensitivity matrix A. The first designated variation pattern contains 42% of the variation; the second 37% and the third one contains 21%. The first designated pattern, see Figure 3.24, seems to correspond to a translation in x-direction, but only in three out of four points. Therefore, this designated pattern cannot be interpreted. The second DC, see Figure 3.25, is also difficult to interpret. The third designated pattern, in Figure 3.26, corresponds to a translation in z-direction in two of the three points evaluated in z-direction.

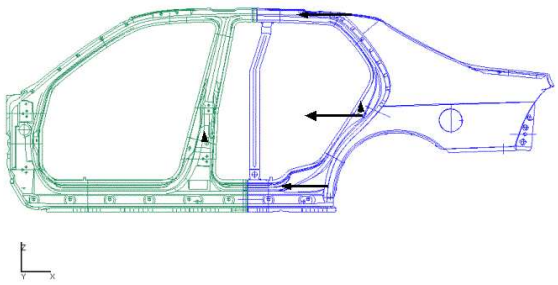

Figure 3.24: *First DC side panel, explains 42% of the variation.*

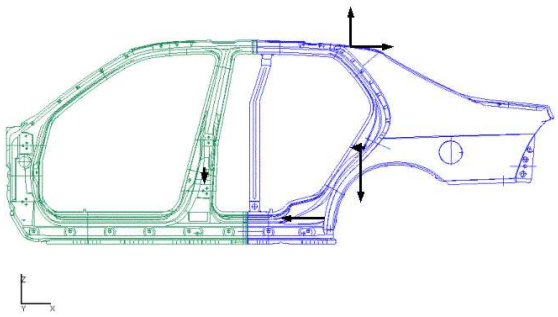

Figure 3.25: *Second DC, side panel assembly, explains 37% of the variation*

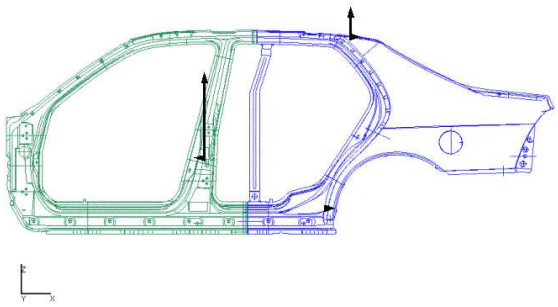

Figure 3.26: *Third DC, side panel assembly, explains 21% of the variation.*

After removing the designated components from data, a principal component analysis of the residuals is carried out. This gives the fourth, fifth and sixth designated components. The fourth DC, see Figure 3.27, corresponds to 75% of the variation in the residuals, and is also difficult to interpret.

In the second case study, the bumper assembly, three designated com-

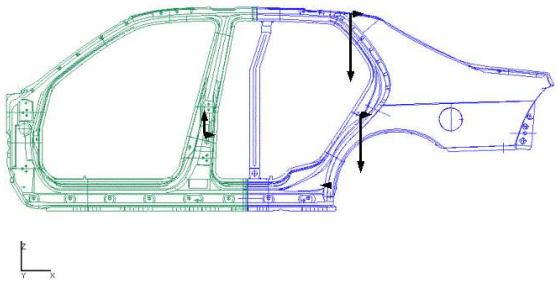

Figure 3.27: *Fourth DC, side panel assembly, explains 75% of the variation in the residuals.*

ponents corresponding to rigid body movements caught by the model were included.

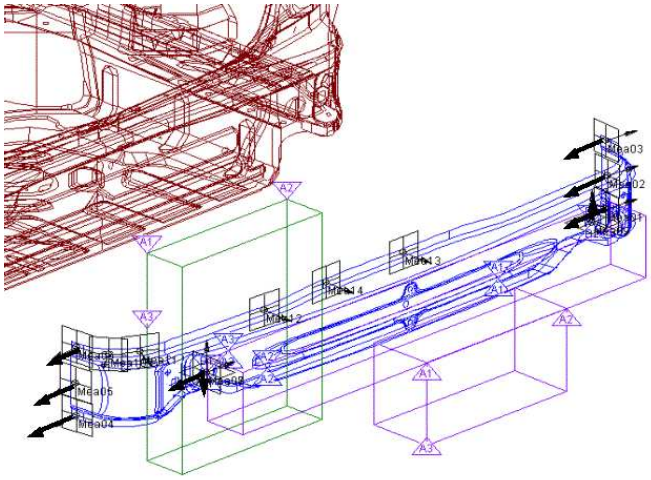

Figure 3.28: *The first designated component, bumper assembly. Contains 38% of the variation.*

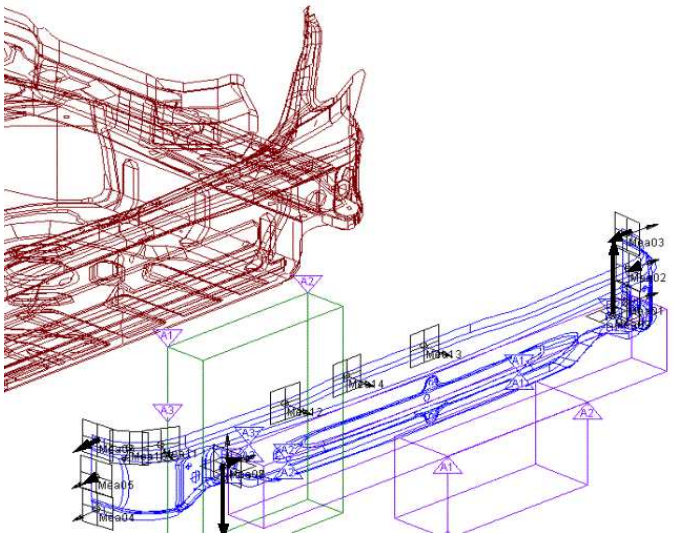

Figure 3.29: *The second designated component, bumper assembly. Contains 37% of the variation.*

The first component shown in Figure 3.28, explains 38% of the variation caught by the model and corresponds mainly to a translation in y-direction. The second component, see Figure 3.29, corresponds to a rotation around the x-axis, just like the third one, Figure 3.30. The second designated component contains 37% of the variation caught by the model and the third one contains 13%.

In the bumper assembly the DCA method points out translation in y-direction as a major root cause, just like the other methods tested. Some kind of rotation around the x-axis is incorrectly pointed out by DCA. When it comes to the side panel assembly there is no obvious interpretation of the results. The first DC seems to mainly correspond to a translation in x-direction, but only in three out of four inspection points. The second DC gives contradictory results, just like the third.

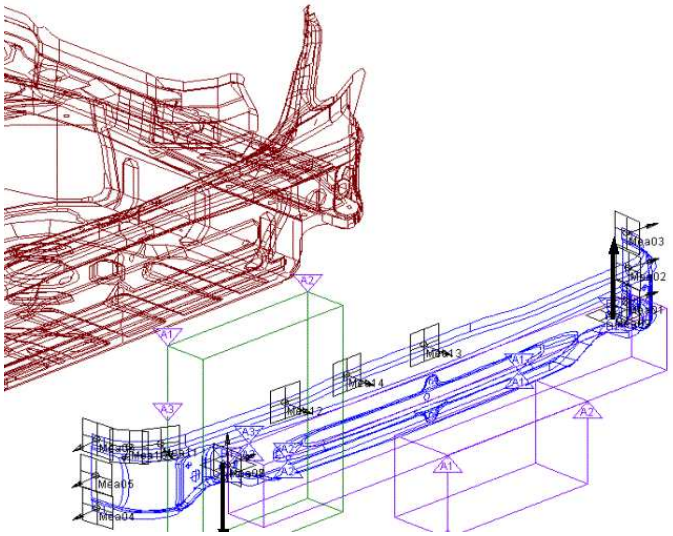

Figure 3.30: *The third designated component, bumper assembly. Contains 13% of the variation.*

3.5 RCA on another case study

Among the methods for diagnosis that was tested, the RCA described by Carlson and Söderberg (6) gives the most easily interpreted result. This method gave also the best agreement with the corrections known to be done in the bumper assembly. On the other hand, there is need of much information about the assembly considered. In this section this method will be further tested on industrial data in order to evaluate its usefulness.

3.5.1 The assembly

The assembly considered is a rear wheelhouse. The wheelhouse consists of five parts and is assembled in two stations. In the first station the wheelhouse panel is positioned and three different reinforcements are assembled to the panel, see left part of Figure 3.31. As shown in the right part of Figure 3.31 this subassembly is then put together with the last part of the rear wheelhouse, namely the support for the parcel shelf. Finally, the complete

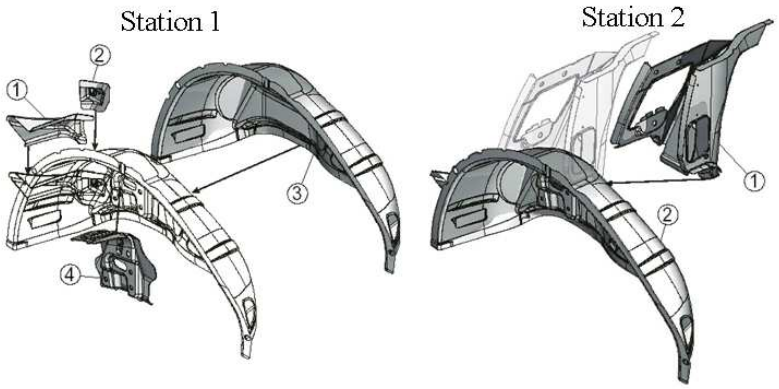

Figure 3.31: *In station one three reinforcements are assembled to the wheelhouse panel. In station two the subassembly from station one is put together with the support for the parcel shelf.*

wheelhouse is measured in an inspection station. It is important to note that the subassembly from station one is positioned in station two using the locators of the wheelhouse panel. This is also the case when the wheelhouse is measured; the locators used can be seen in Figure 3.32. Using those locators results in that a variation in the contact between locator and wheelhouse panel in station one will never be seen as a variation in the

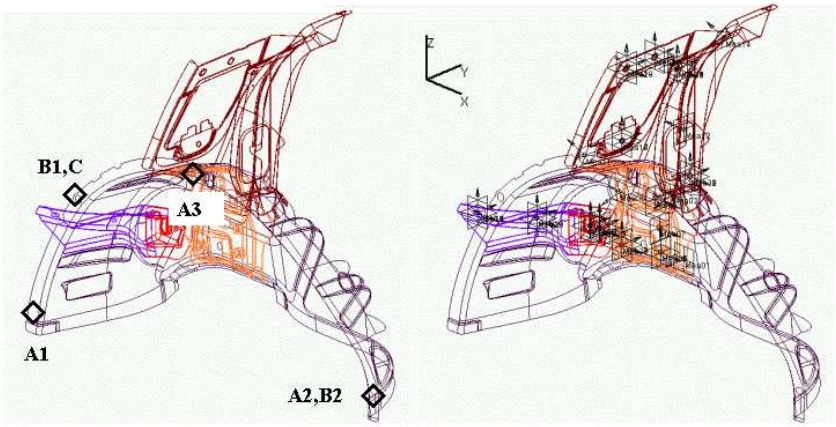

Figure 3.32: *To the left: The locators used to position the subassembly during inspection. To the right: The inspection points are illustrated by arrows.*

inspection points at the wheelhouse panel. Instead, this variation appears in the inspection points situated on the reinforcements that are joined to the panel in the first station. If there is variation in the contacts between the locators and the panel in the second station, this will result in variation in the inspection points on the parcel shelf support. In the right part of Figure 3.32 the 38 inspection points utilized for analysis are illustrated.

RCA is a method that demands knowledge about the sensitivity matrix A, describing the relation between movements in inspection points and movements in the contact between locators and parts. In this case the sensitivity matrix is determined by using simulations in a program called "Robust Design and Tolerancing" (RD&T). It is necessary to describe how every included part is positioned and if the position is completely determined by the fixture or if the mating part positions the part in some direction. The coordinates of the inspection points are also required.

3.5.2 Inspection data

The complete wheelhouse assembly is measured using a coordinate measurement machine. Totally, 38 inspection points are used in the analysis. There are 14 samples of wheelhouses, where each sample consists of three consecutive parts. The inspection data can be seen in Figure 3.33.

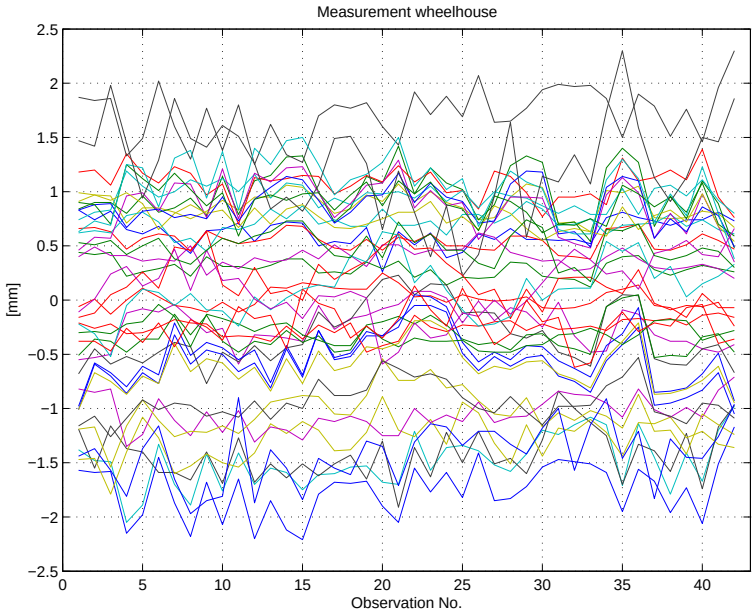

Figure 3.33: *Measurements of 42 wheelhouses in 38 inspection points. Deviations from nominal value are measured.*

The inspection data can be influenced by a lot of different sources of variation. Some of the variations are long-term variations, which slowly change the process over time, for example variations due to changes in raw material or wear in tools. To avoid mixing up these sources of variation with variation caused by the fixtures, only within samples variation is considered. This is logical since if there is fixture related variation, this variation will affect every produced item, and consequently also contribute to the variation within every sample.

In order to decide if the variation in data can be a consequence of variation in the contacts between parts and locators, the fixture fault variation

index is determined. The index is calculated for each sample, see Figure 3.34. Since the index is above the line corresponding to the value of Ψ when

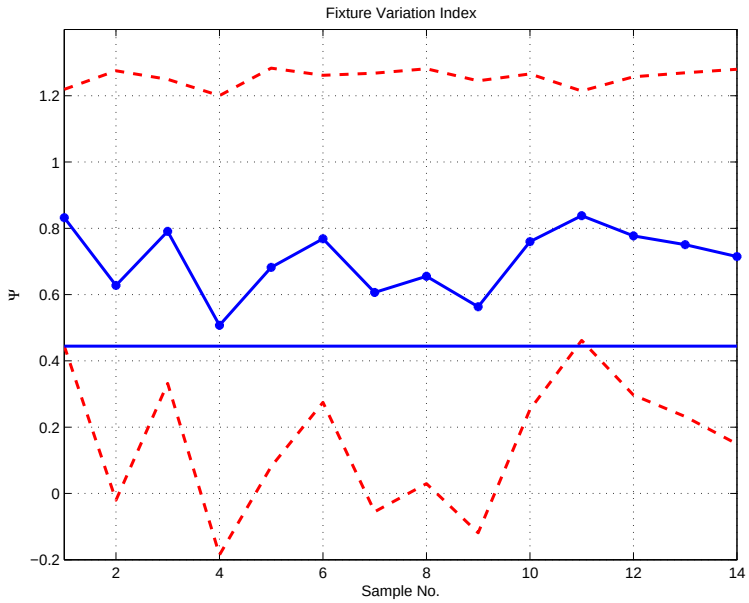

Figure 3.34: *Fixture fault variation index for 14 samples.*

there is no fixture fault, it seems reasonable to continue with the root cause analysis.

3.5.3 Root Cause Analysis

To conclude what fixture or fixtures that caused the variation, the variation in the contact between parts and locators are estimated using inspection data. This is done for most of the locators. Some locators are though excluded. The reason is that it otherwise would be necessary to use more inspection points in order to carry out a complete analysis.

In Figure 3.35 are the estimated variances shown. As seen, the major source of variation is the contact between the locator called B2 and the wheelhouse panel in the first station. The locator B2 consists of a pin in a slot and position the wheelhouse panel in z-direction, see Figure 3.36.

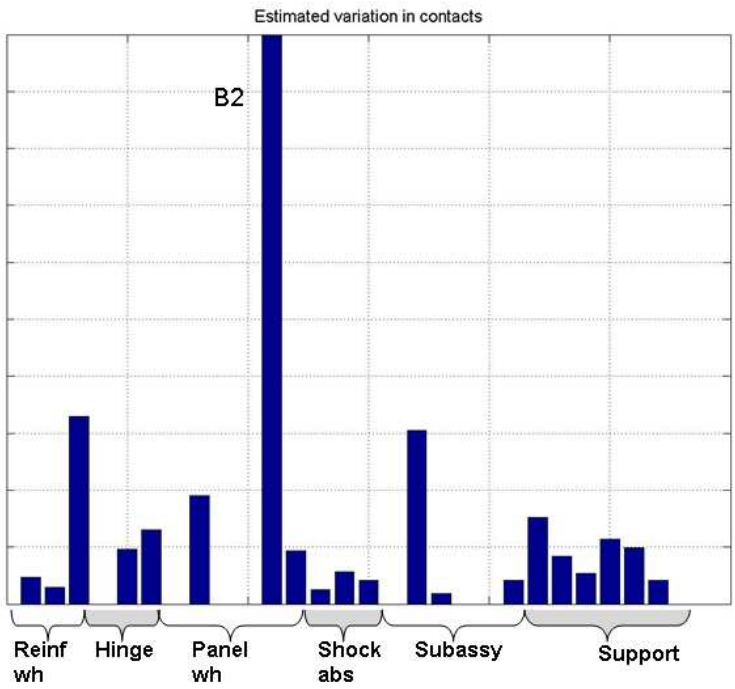

Figure 3.35: *Estimated variance in the contacts between parts and locators.*

3.5.4 Adjustment of the fixture

RCA is a tool for identifying the fixture related sources of variation in a process. When this identifying is done, the result should be translated into an adjustment of the fixtures. It is though important to note that RCA gives no outline for this adjustment. The work of doing the adjustment should be done by someone with good knowledge of the process and a good understanding about how different kinds of locators affect the positioning of parts.

Since the contact between the wheelhouse panel and the locator B2 was pinpointed as a major source of variation this locator is adjusted. The adjustment consists of changing the pin in B2 to an egg-shaped pin corresponding to the shape of the slot. After this modification 24 complete wheelhouses are measured. Unfortunately, this adjustment did not reduce

Figure 3.36: *The contact B2 in station 1 is a major source of variation.*

the variation. The variation in the inspection points situated on the reinforcements assembled in station one increased, see Figure 3.37. As mentioned before, variation in the positioning of the wheelhouse panel in station one, will give rise to variation in the inspection points on the reinforcements assembled to the panel in station one. The reason is that the wheelhouse assembly is positioned using the locators of the panel in the inspection station.

The adjustment lead to increased variation in the inspection points, but it is still of interest to analyse the inspection data after the adjustment to estimate the corresponding variation in contacts between parts and locators. In Figure 3.38 is the estimated variation before and after the adjustment shown. Here, the locators in station two are excluded, since they are not involved in the adjustment.

From Figure 3.38 it can be seen that the variation in the contact between the part and the adjusted locator B2 undoubtedly has increased. The variation has also increased in the contact between the panel and the locator A2. This locator is situated just beside B2, and position the panel in y-

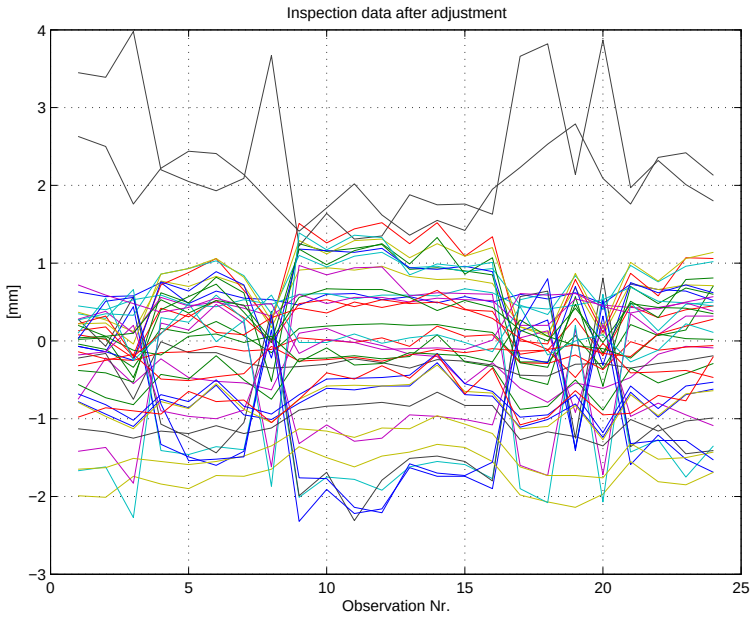

Figure 3.37: *Inspection data after the adjustment.*

direction.

3.5.5 Conclusions of the case study

Since the adjustment of the fixtures is well known it is a very good case for testing the method. In this case the variation increased, but the important thing is that the locator corresponding to these increased variation could be pinpointed by using RCA.

If the case would have been the reversed, i.e. there would have been much variation because of an unsuitable positioning element (like B2 after the adjustment), the method could have been used to pinpoint the source of the variation and is thereby a tool for reducing the variation.

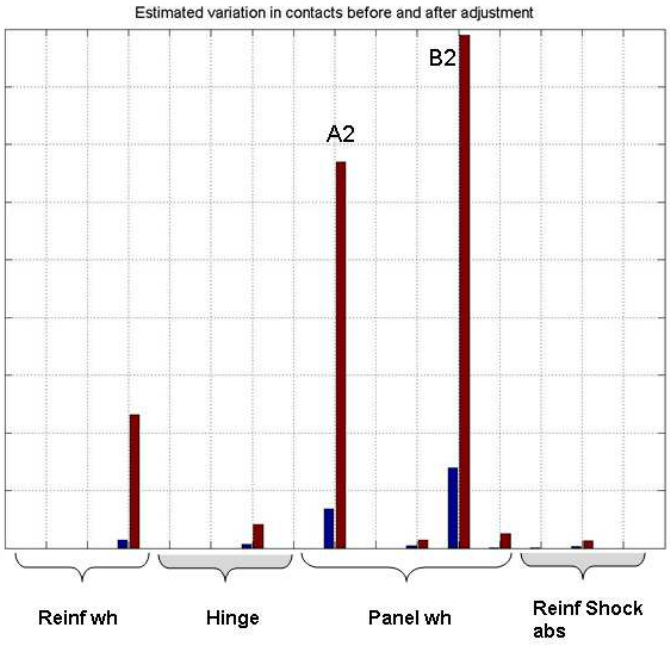

Figure 3.38: *For each locator the left bar corresponds to estimated variation in the contact between part and locator before adjustment, and the right bar corresponds to estimated variation after the adjustment.*

3.6 Discussion and conclusions

Different methods for as well multivariate quality control as diagnosis have been tested on the case studies. Both case studies turned out to be out of statistical control. The second case study, the bumper assembly, was in advance known to be out of control due to a fixture failure occurring after 16 measurements. This fixture failure occurred as a result of a defect locator in y-direction. No prior information of fault or fault types were available when it comes to the side panel assembly, but the result from different methods can still be compared.

3.6.1 Process control

The T^2-chart is one of the most popular multivariate charts and it works satisfyingly on the case studies. It detects quickly the change in the process of the bumper assembly. The covariance matrix for the inspection data is though nearly singular. This affects the T^2-statistic and may in some cases lead to misinterpretations. When it comes to the side panel assembly there are several alarms even though trends in data are eliminated. The T^2-chart requires no advanced calculations and is easy to use. A disadvantage is that the chart gives no indication of which inspection points that caused an alarm. The chart is also based on the assumption that data is normally distributed.

The PCA- and SPE-chart is similar to the T^2-chart but operates in the subspace spanned by the principal components. This means that the dimension of data is reduced, but in the same time some information is lost. In addition there is need of two charts, both the T^2_{pca} and the SPE-chart. The PCA/SPE chart alarms after the change in the bumper assembly process, nevertheless there is a delay compared to the T^2-chart. The PCA-chart are, unlike the usual T^2-chart, not affected by singularity in the covariance matrix.

Regression adjustment differs from the other charts. This method can be used for controlling mean and variance separately, which is an advantage. However, this is also possible to achieve by using a T^2-chart complemented by a multivariate chart for controlling within group variation. However, such a chart can be complicated to use when the data are ungrouped. The regression adjustment chart is suitable when only a few of the variables are expected to change. However, this is usually not the case if the fault is caused by fixture fault. This property makes this chart unsuitable for controlling the process from the case studies. Using this chart it is necessary

to generate one chart for each variable, but on the other hand this chart indicates what variable causing an alarm.

To train a SOM there is need of much data, but there is no need of assumptions on distribution of the data. In some cases the SOM helps finding the root cause of an erroneously state.

The fixture fault index and the fixture fault chart are both aimed to detect fixture related faults. For both methods there is need to know the so called A-matrix, the sensitivity matrix relating a movement in the locators to a corresponding movement in the inspection points. The methods are also intended for normally distributed data. The fixture fault index is useful when it comes to find the root cause of a variation. If the index is high a fixture probably caused the fault and the main efforts can be concentrated to examining the fixtures. The methods work well on the case studies.

Method	Panel ass.	Bumper ass.	Remarks
T^2-chart	5 alarms	Alarm after mea 16	Sensitive to S almost singular
T^2_{PCA}/SPE	3 alarms	Alarm after mea 16	Not sensitive to S almost singular
Reg. adj.	Many alarms	Alarms, but no obvious change after mea 16	Most suitable when few variables change
SOM	Not tested	Obvious change after mea 16	No assumptions about distribution
Fixture index	Many alarms	Alarms, obvious change after mea 16	Specialized for controlling fixture faults
$T^2_{fixture}$/SPE	Many alarms	Alarms, obvious change after mea 16	Specialized for controlling fixture faults

Figure 3.39: *A comparison of the different methods used for multivariate quality control.*

In Figure 3.39 the performances of the different charts are tabulated.

3.6.2 Fixture fault diagnosis

When it comes to finding the cause of the fixture fault there are two main methods, namely the RCA and the both visual methods PCA and DCA. The RCA is more complex then the PCA and DCA methods. On the other hand the result is clear and easy to interpret. In the PCA-method there is no need of the sensitivity matrix A, which is demanded in the RCA and DCA methods. For both PCA and DCA the calculation is simple, but the interpretation of the result is not always trivial. The DCA is similar to the PCA, but is specialized to find fixture faults. A drawback of DCA compared to PCA is that the sensitivity matrix is needed.

When applying the methods to the case studies the RCA identified the failing locator in the bumper assembly. This is a locator in y-direction and also the PCA and the DCA show translation in y-direction as a main problem. In this case there is only one locator in y-direction and this locator is consequently pointed out as the main cause of the variation. If there would have been several locators in y-direction, it might have been hard to separate them using the visual methods. The DCA does also incorrectly point out rotation around the x-axis as a root cause.

In the side panel assembly a pin/hole contact in z-direction located in the front of the doorframe is pointed out as the root cause by the RCA. This is confirmed by the PCA, where the first eigenvector corresponds to a translation in z-direction. This translation is though combined with a rotation. The designated components are very difficult to interpret and seem to give contradictory results. The multi-fixture side panel assembly is not completely diagnosable and both the visual methods PCA and DCA are very hard to interpret.

To sum up, PCA and DCA is easy to calculate and when using the PCA there is no need to know the sensitivity matrix A. However, the methods seem to be best suited for identifying single locator fault in small completely diagnosable assemblies. The RCA is a more versatile method that gives more exact results. However, to use this method the sensitivity matrix must be known.

Bibliography

[1] J. Ahola, E. Alhoniemi, and O. Simula. Monitoring industrial processes using the self-organizing map. In *Midnight-Sun Workshop on Soft Computing Methods in Industrial Applications*, Kuusamo, Finland, June 1999. IEEE.

[2] F. B. Alt. Multivariate quality control: State of the art. In *Transactions of the 1982 ASQC Quality Congress*, pages 886–893, 1982.

[3] J. A. Camelio and S. J. Hu. Multiple fault diagnosis for sheet metal fixtures using designated component analysis. *Journal of Manufacturing Science and Engineering*, 126, February 2004.

[4] J. S. Carlson, L. Lindkvist, and R. Söderberg. Multi-fixture assembly system diagnosis based on part and subassembly measurement data. In *Proceedings of the ASME Design Engineering Technical Conferences, Baltimore*, 2000.

[5] J. S. Carlson and R. Söderberg. Locating scheme analysis for robust assembly & fixture design. In *Proceedings of the ASME Design Engineering Technical Conferences, Las Vegas*, 1999.

[6] J. S. Carlson and R. Söderberg. Assembly root cause analysis - a way to reduce dimensional variation in assembled products. *International Journal of Flexible Manufacturing Systems*, 15(2):113–150, April 2003.

[7] J. S. Carlson, R. Söderberg, and L. Lindkvist. Geometrical inspection point reduction based on combined cluster and sensitivity analysis. In *Proceedings of the ASME International Mechanical Engineering Congress & Exposition, Washington D. C.*, 2003.

[8] D. L. Ceglarek and J. Shi. Dimensional variation reduction for automotive body assembly. *Manufacuring Review*, 8(2):139–154, 1995.

[9] T. C. Chang and F. F. Gan. Application of $\bar{x}$ control chart with modified limits in process control. *Quality and Reliability Engineering International*, 15:355–362, 1999.

[10] H. Chen. A multivariate process capability index over a rectangular solid tolerance zone. *Statistica Sinica*, 4:749–758, 1994.

[11] Y. Ding, A. Gupta, and D. Apley. Singularity issues in fixture fault diagnosis for multi-station assembly processes. *ASME Transactions, Journal of Manufacturing Science and Engineering*, 126(1), February 2004.

[12] M. D. Hawkins. Regression adjustment for variables in multivariate quality control. *Journal of Quality Technology*, 25(3), 1993.

[13] S. Haykin. *Neural Networks*. Prentice Hall, 2nd edition, 1999.

[14] A. J. Hayter and K-L. Tsui. Identification and quantification in multivariate quality control problems. *Journal of Quality Technology*, 26(3):197–208, 1994.

[15] S.D. Holmes and A. E Mergen. Exponentially weighted moving average acceptance control chart. *Quality and Reliability Engineering International*, 16:139–142, 2000.

[16] H. H. Hotelling. Multivariate quality control illustrated by the air testing of sample bombsights. *Techniques of Statistical Analysis*, pages 111–184, 1947.

[17] S. J. Hu and S. M. Wu. Identifying sources of variation in automobile body assembly using principal component analysis. In *Transactions of NAMRI/SME*, 1992.

[18] J. E. Jackson. Principal components and factor analysis: Part 1 - principal components. *Journal of Quality Technology*, 12:201–213, 1980.

[19] J. E. Jackson. Multivariate quality control. *Communication in Statistics - Theory and Method*, 14(11), 1985.

[20] J. E. Jackson. *A User's Guide To Principal Components*. John Wiley & Sons, New York, 1991.

[21] R. A. Johnson and D. W. Wichern. *Applied Multivariate Statistical Analysis*. Prentice-Hall, 1998.

[22] K. G Jöreskog. Analysis of covariance structures. *Scandinavian Journal of Statistics*, 8:65–92, 1981.

[23] T. Kohonen. *Self-Organizing Maps.* Springer, New York, 3rd edition, 2000.

[24] L. Lindkvist and R. Söderberg. Computer-aided tolerance chain and stability analysis. *Journal of Engineering Design*, 14(1):17–39, March 2003.

[25] D. C. Montgomery. *Introduction to Statistical Quality Control.* John Wiley and Sons, 4rd edition, 2001.

[26] G. C. Runger, F. B. Alt, and D. C. Montgomery. Contributors to a multivariate statistical process control chart signal. *Communication in Statistics - Theory and Methods*, 25(10):2657–2213, 1996.

[27] Saab standard no. 3546.

[28] Saab standard no. 3581.

[29] H. Shahriari, N. F. Hubele, and F. P. Lawrence. Multivariate process capability vector. In *Proceedings of the 1995 4th Industrial Engineering Research Conference.* IEE, May 1995.

[30] R. Söderberg and L. Lindkvist. Computer aided assembly robustness evaluation. *Journal of Engineering Design*, 10(2):165–181, 1999.

[31] R. Söderberg and L. Lindkvist. Two-step procedure for robust design using cat technology. In *6th CIRP International Seminar on Computer Aided Tolerancing*, Enschede, the Nederlands, March 1999.

[32] W. Taam, P. Subbaiah, and J. W. Liddy. A note on multivariate capability indices. *Journal of Applied Statistics*, pages 339–351, 1993.

[33] G. Taguchi. *Introduction to Quality Engineering.* Asian Productivity Centre, 1986.

[34] A. Ultsch and H. P. Siemon. Kohonen's self organizing feature maps for exploratory data analysis. In *Proc. Int. Neural Network Conf. Dordrecht, The Netherlands*, 1990.

[35] F.K Wang, N. F. Hubele, F. P. Lawrence, J. D. Miskulin, and H. Shahriari. Comparison of three multivariate process capability indices. *Journal of Quality Technology*, 32(3):263–275, 2000.

[36] G. B. Wetherhill and D. W. Brown. *Statistical Process Control, Theory and practice.* Chapman & Hall, 1 edition, 1990.

[37] C. Wickman and R. Söderberg. Comparasion of non-nominal geometry models represented in physical versus virtual environments. In *Proceedings of IMECE'03 ASME International Mechanical Engineering Congress & Exposition*, Washington D.C., November 2003.

[38] W. H Woodall. Controversies and contradictions in statistical process control. *Journal of Quality Technology*, 32(4), 2000.